BJ www.biochemj.org

BJ Signal

Biochem. J. (2008) **416**, 1–14 (Printed in Great Britain) doi:10.1042/BJ20081447

online data online commentary

A novel short splice variant of the tumour suppressor LKB1 is required for spermiogenesis

Mhairi C. TOWLER*, Sarah FOGARTY*, Simon A. HAWLEY*, David A. PAN*[2], David M. A. MARTIN†, Nicolas A. MORRICE‡, Afshan McCARTHY§, María N. GALARDO‖, Silvina B. MERONI‖, Selva B. CIGORRAGA‖, Alan ASHWORTH§, Kei SAKAMOTO‡ and D. Grahame HARDIE*[1]

*Division of Molecular Physiology, School of Life Sciences, University of Dundee, Dow Street, Dundee DD1 5EH, Scotland, U.K., †Post-Genomics and Molecular Interactions Centre, College of Life Sciences, University of Dundee, Dundee DD1 5EH, Scotland, U.K., ‡MRC Protein Phosphorylation Unit, College of Life Sciences, University of Dundee, Dundee DD1 5EH, Scotland, U.K., §The Breakthrough Breast Cancer Research Centre, The Institute of Cancer Research, Fulham Road, London SW3 6JB, U.K., and ‖Centro de Investigaciones Endocrinológicas (CEDIE-CONICET), Hospital de Niños "R. Gutiérrez", Gallo 1330, C1425EFD Buenos Aires, Argentina

LKB1 was discovered as a tumour suppressor mutated in Peutz-Jeghers syndrome, and is a gene involved in cell polarity as well as an upstream protein kinase for members of the AMP-activated protein kinase family. We report that mammals express two splice variants caused by alternate usage of 3′-exons. $LKB1_L$ is the previously described form, while $LKB1_S$ is a novel form in which the last 63 residues are replaced by a unique 39-residue sequence lacking known phosphorylation (Ser^{431}) and farnesylation (Cys^{433}) sites. Both isoforms are widely expressed in rodent and human tissues, although $LKB1_S$ is particularly abundant in haploid spermatids in the testis. Male mice in which expression of $Lkb1_S$ is knocked out are sterile, with the number of mature spermatozoa in the epididymis being dramatically reduced, and those spermatozoa that are produced have heads with an abnormal morphology and are non-motile. These results identify a previously undetected variant of LKB1, and suggest that it has a crucial role in spermiogenesis and male fertility.

Key words: AMP-activated protein kinase (AMPK), LKB1, male fertility, spermiogenesis, splice variants.

INTRODUCTION

The *LKB1 (STK11)* gene, encoding a tumour suppressor protein kinase, was discovered as the gene mutated in human PJS (Peutz-Jeghers syndrome), a cancer predisposition that is inherited in an autosomal dominant manner [1,2]. PJS subjects develop numerous benign polyps in the gastrointestinal tract and have a 20-fold increased risk of developing malignant tumours at other sites, while mutations in the *LKB1* gene are also seen in some sporadic cancers, especially adenocarcinoma of the lung [3]. Several human tumour cell lines lack LKB1, and expression of the protein in these cells causes a G_1 cell cycle arrest. Homozygous $Lkb1^{-/-}$ knockout mice die at mid-gestation, while heterozygous mice develop intestinal lesions similar to those found in humans with PJS [3]. Thus analysis of heterozygous mutations in mammalian species suggest that LKB1 has a role in restraining cell growth and proliferation. Genetic studies in other eukaryotes such as *Caenorhabditis elegans* and *Drosophila melanogaster* have suggested another function, i.e. that LKB1 has a role in the establishment and/or maintenance of cell polarity. In *C. elegans,* a maternal effect lethal mutation in the LKB1 orthologue, *par-4*, disrupts the normal asymmetry in the first cell cycles of embryogenesis [4]. Mutations in the *D. melanogaster* orthologue, dLKB1, cause defects in cell polarity in the oocyte and the developing embryo [5,6].

Important insights into the biochemical function of LKB1 came with the discovery that it is an upstream kinase that phosphorylates the activation loop of protein kinases of the AMPK (AMP-activated protein kinase) family. These include the α1 and α2 isoforms of AMPK itself [7–9], as well as at least 12 AMPK-related kinases [10,11]. AMPK exists as heterotrimeric complexes formed from catalytic α subunits and regulatory β and γ subunits, each of which has multiple isoforms encoded by distinct genes [12]. LKB1 phosphorylates Thr^{172} on the catalytic α subunits of AMPK, and the equivalent threonine on the AMPK-related kinases, causing in every case a pronounced activation. Whether activation of AMPK accounts for the tumour suppressor properties of LKB1 remains uncertain. However, AMPK activation inhibits the TOR (target of rapamycin) pathway [13,14], thus inhibiting cell growth, and also causes a $G_1 \rightarrow$ S-phase cell cycle arrest in cultured cells, an effect that involves increased phosphorylation of p53 [15,16]. Also consistent with the idea that AMPK mediates the tumour suppressor functions of LKB1 are findings that the TOR pathway is hyperactive in intestinal lesions from $Lkb1^{+/-}$ heterozygous mice [17], and that pharmacological activators of AMPK reduce tumour formation in a cancer-prone mouse model that is heterozygous for PTEN (phosphatase and tensin homologue deleted on chromosome 10) and has a hypomorphic mutation in LKB1 [18].

The role of LKB1 in establishment of cell polarity may also involve activation of AMPK, because null mutations in the LKB1 and AMPK genes in *D. melanogaster* cause similar defects in polarity of epithelial cells in the developing embryo [6]. Activation of either LKB1 or AMPK in cultured intestinal or

Abbreviations used: AMPK, AMP-activated protein kinase; DAPI, 4′,6-diamidino-2-phenylindole; DMEM, Dulbecco's modified Eagle's medium; DTT, dithiothreitol; EM, electron microscopy; EST, expressed sequence tag; GST, glutathione transferase; HBSS, Hanks balanced salt solution; HEK cell, human embryonic kidney cell; MALDI–TOF, matrix-assisted laser-desorption ionization–time-of-flight; MARK, microtubule affinity-regulating kinase; MO25, mouse protein 25; NUAK, sucrose-non-fermenting kinase-1 (SNF1)-like kinase; PJS, Peutz-Jeghers syndrome; QIK, Qin-induced kinase; RACE, rapid amplification of cDNA ends; RT–PCR, reverse transcription–PCR; SIK, salt-inducible kinase; SNARK, SNF1/AMP-activated protein kinase; SNF, sucrose-non-fermenting kinase; STRAD, Ste20-related adaptor; TOR, target of rapamycin.

[1] To whom correspondence should be addressed (email d.g.hardie@dundee.ac.uk).
[2] Present address: Prosidion Limited, Windrush Court, Watlington Road, Oxford OX4 6LT, U.K.

kidney epithelial cells also triggers establishment of cell polarity [6,19–21]. However, several of the kinases downstream of LKB1 also appear to have functions in cell polarity, including the MARKs (microtubule affinity-regulating kinases) [22], which are homologues of *C. elegans* PAR-1, and BRSK1/BRSK2 (SAD-B/SAD-A) [23], which are homologues of *C. elegans* SAD-1.

LKB1 exists *in vivo* as a complex with two accessory subunits, i.e. STRAD (Ste20-related adaptor), which is essential for LKB1 activity, and MO25 (mouse protein 25), which appears to stabilize the LKB1–STRAD complex [3]. At least 75 mutations affecting the amino acid sequence of LKB1 have been found in PJS subjects and in sporadic cancers. Most either directly interfere with the kinase activity, or abolish it indirectly by preventing interaction with STRAD. However, a significant number (approx. 20 %) affect the C-terminal region of LKB1, where they do not appear to affect kinase activity or STRAD interaction [3].

In this study, we report that the C-terminal region of LKB1 is affected by alternative splicing to produce long and short variants of the LKB1 polypeptide ($LKB1_L$ and $LKB1_S$) that have different C-terminal sequences. $LKB1_S$, which lacks the Ser^{431} phosphorylation site and the farnesylation site, is a minor form in most tissues but is highly abundant in haploid spermatids in the testis. Both $LKB1_L$ and $LKB1_S$ are capable of activating AMPK and all of the AMPK-related kinases tested. However, male mice that cannot generate $Lkb1_S$ are sterile and produce dramatically reduced numbers of mature spermatozoa that are non-motile and have abnormal morphology.

MATERIALS AND METHODS

Cloning and expression of rat $LKB1_S$ and $LKB1_L$ and other plasmids

Based on a rat EST (expressed sequence tag) (BF396918) that encoded the last 11 amino acids of $LKB1_L$ followed by a 3′-UTR and poly(A) tail, we designed a reverse primer (5′-TGGCGACACACTGTTGGTAGAATG-3′), whereas the forward primer (5′-GAACTTGAAAAGAATTGGCGCTCC-3′) was based on a sequence 50 bp upstream of the initiator ATG codon in rat, based on results of 5′-RACE (rapid amplification of cDNA ends). These were used to generate full-length rat $LKB1_L$ DNA by RT–PCR (reverse transcription–PCR) using the Titan One Tube RT–PCR kit (Roche Diagnostics) with the rat brain RNA as template. The product was gel purified, ligated into pGEM-T Easy (Promega), and used to transform TOP10F' *Escherichia coli*. Colonies were picked and it was confirmed that they contained the full-length rat $LKB1_L$ sequence. A 1700 bp EcoRI/SpeI fragment was ligated into pcDNA3.1/Zeo. Searching the NCBI database revealed a rat testis EST (CK597755) that encoded the C-terminal region of $LKB1_S$ plus 52 bp of 3′-UTR and a poly(A) tail. This was purchased from the IMAGE consortium. The insert was $\approx$1700 bp, and sequencing revealed that it encoded the full-length $LKB1_S$ sequence. The insert was also sub-cloned into pcDNA3.1/Zeo. For the GST (glutathione transferase) fusions, $LKB1_L$ and $LKB1_S$ DNAs were amplified from the pcDNA3.1 vectors for subcloning into pEBG2T as a Spe1-Kpn1 insert using the forward primer 5′-CGGACTAGTCCGATGGACGTGGCTGACCCCCAG-3′ and reverse primers 5′-CGGGGTACCCCGTCACTGCTGCTTGCAGGCCGA-3′ ($LKB1_L$) or 5′-CGGGGTACCCCGTCACAGTGGACAAAGCTTTAT-3′ ($LKB1_S$).

Antibodies

The anti-LKB1(N) antibody was raised against the peptide TFIHRIDSTEVIYQP (residues 24–36 of human, mouse and rat LKB1) [24]. Although raised against the peptide phosphorylated on Ser^{31}, the antibody was affinity purified on a column containing the dephosphopeptide (with an N-terminal cysteine, coupled via the thiol group to CH-Sepharose 4B (Pharmacia) as described previously [25]). The purified antibody does not appear to be dependent on the phosphorylation state of Ser^{31} because it recognizes an S31A mutant as well as wild-type LKB1. The anti-$LKB1_L$ antibody was raised in sheep against the peptide KIRRLSACKQQ (residues 423–436 of rat $LKB1_L$, with a farnesyl group on Cys^{433}), and was affinity purified on a column containing the defarnesylated peptide. Although this antibody was raised in an attempt to develop an antibody that was dependent on farnesylation status, when purified in this manner it appeared to be farnesylation-independent, because it recognized an C433A mutant as well as wild type $LKB1_L$. The anti-$LKB1_S$ antibody was raised in sheep against the peptide CGLPGEEPEEGFGAVV (residues 398–412 of rat $LKB1_S$ plus N-terminal cysteine) using methods described previously [25]. MARK3 antibodies were from Upstate Biotech (#05–680) and anti-pT172 and anti-*myc* antibodies from Cell Signaling Technology (#2535L and #2276). Antibodies against SIK1 (salt-inducible kinase 1) (SIK), SIK2 [QIK (Qin-induced kinase)], SIK3 (QSK), NUAK2 [sucrose-non-fermenting kinase-1 (SNF1)-like kinase 2] and MARK1 [10], AMPK-α1 and -α2 [26], GST [27], and a monoclonal antibody against STRADα were as described previously [28].

Bioinformatic analysis of LKB1 sequences

LKB1 peptide sequences [Q15831, human; Q9WTK7, mouse; XP_234900, rat (two versions)] were obtained from the Uniprot and RefSeq databases using a keyword search, and used as probes to search the human, mouse and rat genome databases at ensEMBL. A strong hit was noted for LKB1 in each genome on chromosome 19 (human), 10 (mouse) and 7 (rat). Each LKB1 sequence was aligned against the respective genomic sequence using EXONERATE (http://www.ebi.ac.uk/~guy/exonerate/) and putative intron/exon boundaries identified for $LKB1_L$ in rat, mouse and human. Alignment of the sequence for rat $LKB1_S$ allowed the putative intron/exon boundaries for intron 8 to be identified in rat and mouse. The human sequence for exon 9A shows only partial similarity to rat and mouse and was not identified by this method. Instead, rat exon 9A sequence, as verified through EST evidence (see below) was aligned with the human genomic sequence using TBLASTN, and the putative intron/exon boundaries identified by manual inspection of the location of the short match in the context of three frame translations and splice sites.

Intron/exon boundaries were verified by alignment of EST sequences with the genomic sequence for all three species. BLAST [29] searches of dbEST using the protein sequences and fragments of the genomic sequence identified EST sequences corresponding to full coverage of all forms of the protein in all species. At least two ESTs were found for each form of the protein in each species. The EST sequences were manually aligned with the genomic sequence using the Jalview multiple sequence alignment editor [30]. There is an additional intron (intron 10) in the mRNA coding for the long form of the protein, 3′ to the translation stop codon, which is conserved across all three species.

RACE

The 3′-RACE was carried out using the Marathon cDNA Amplification Kit (Clontech), using Marathon Ready rat testis cDNA (Clontech Cat. #639417) as template. 3′-RACE was carried out using the forward gene-specific primer TTGACGGCCTGGAGTACCTACACA (encoding residues 161–168 in the

common region). This gave rise to two products, a major product of 830 bp and a minor product of approx. 560 bp. These were gel purified and re-amplified by a second round of PCR. Sequencing of the 830 bp product using the primer GAGTACGAGCCAGCCAAGAG yielded a sequence encoding residues 330–412 of $LKB1_S$. Sequencing of the 560 bp product using the primer GTCACACTCTACAACCATCACCACG yielded a sequence encoding residues 291–406 of $LKB1_L$.

Immunoprecipitation of rat testis LKB1 and analysis by mass spectrometry

LKB1 was purified to the Q-Sepharose stage from rat testis as described previously for rat liver [7] and fractions containing both $LKB1_L$ and $LKB1_S$ were identified by Western blotting. These fractions (3.75 mg of protein) were immunoprecipitated using antibody against GST–LKB1 [31] covalently conjugated to Protein G–Sepharose using dimethylpimelimidate [32]. After extensive washing, bound protein was eluted using 1 % SDS in 20 mM Tris/HCl, pH 7.5. Samples were concentrated 10-fold using a Speedivac concentrator, and protein was precipitated overnight using 10 vol. of ice-cold methanol. After centrifugation (16 000 ***g***, 15 min) the precipitate was resuspended in SDS sample buffer, proteins were resolved by SDS/PAGE on a 4–12 % precast gradient gel using the Mops buffer system (Invitrogen) and visualized by staining with colloidal Coomassie Blue. Stained polypeptides were destained, digested with trypsin and analysed by MS using an Applied Biosystems 4700 Proteomics Analyser [33]. Digests were also analysed by LCMS (liquid chromatography-electrospray MS) using an Applied Biosystems 4000 Q-TRAP mass spectrometer [34].

Immunoprecipitation and Western blotting of LKB1 from various tissue extracts

Male rats (Wistar) or mice were anaesthetized using CO_2 and killed by cervical dislocation. Animals were killed by approved humane methods. Procedures involving live animals were subject to the Animals (Scientific Procedures) Act 1986 (U.K.) and were approved by the institutional ethical committee. The indicated tissues were rapidly removed, frozen in liquid N_2 and stored at −80 °C until used. Tissue samples were pulverized under liquid N_2 and homogenized in a hand held homogenizer on ice in lysis buffer [50 mM Tris/HCl, pH 7.5, 50 mM NaF, 1 mM sodium pyrophosphate, 1 mM EDTA, 1 mM EGTA, 1 % Triton X-100, 1 mM DTT (dithiothreitol), 0.1 mM PMSF, 1 mM benzamidine and 1 μg/ml soybean trypsin inhibitor]. Homogenates were centrifuged (13 000 ***g***, 15 min, 4 °C), supernatants removed, frozen in liquid N_2 and stored at −80 °C until used. Samples (20 or 200 μg of protein) were incubated at 4 °C for 2 h on a shaking platform with 5 μl of Protein G–Sepharose covalently conjugated (using dimethylpimelimidate) to 10 μg of anti-LKB1(N) antibody. After extensive washing, the immunoprecipitates were heated in SDS sample buffer, resolved by SDS/PAGE and blots were probed with the indicated antibodies.

Human protein medleys (10 mg/ml in SDS sample buffer) from brain, heart, liver and testes were from Clontech. They were resolved by SDS/PAGE without prior immunoprecipitation and analysed by Western blotting with the indicated antibodies.

For Figures 3(D), 6(B) and 6(C), homogenates were prepared from rat or mouse testis and epididymis by grinding tissue under liquid N_2 and adding an equal volume of homogenization buffer (50 mM Tris/HCl, pH 7.3, 1 mM EDTA, 1 mM EGTA, 50 mM NaCl, 5 mM sodium pyrophosphate, 50 mM NaF, 2 mM DTT, 1 mM PMSF, 2 mM benzamidine, 1 % Triton X-100 and 250 mM mannitol) and homogenizing using a Dounce homogenizer. Samples were left on ice for 30 min, followed by a second bout of homogenization before being centrifuged at 21 000 ***g*** (4 °C) and the supernatant used for immunoprecipitation or analysis by Western blotting. For preparation of spermatozoa extract, the epididymis was chopped finely in PBS and centrifuged (3000 rev./min, 2 min, 4 °C). The supernatant was centrifuged again (14 000 rev./min, 4 °C, 5 min). The pellet containing the spermatozoa was lysed in 50 μl of homogenization buffer and left on ice for 30 min, followed by centrifugation (14 000 rev./min, 5 min, 4 °C). The supernatant was analysed by Western blotting.

Isolation of RNA from mouse testis and RT–PCR

RNA was extracted from $LKB1^{+/+}$ and $LKB1^{fl/fl}$ mice testis as follows: 1 ml TRIzol® reagent (Invitrogen) was added to tissue in a tube containing lysing matrix D (small ceramic beads) and placed on ice. Tissue was homogenized using the Precellys 24 machine (Bertin Technologies) at 6000 rev./min twice for 20 s. Tubes were left on ice for 5 min, chloroform (200 μl) was added, tubes were vortexed for 1 min and then centrifuged (21 000 ***g***, 15 min, 4 °C). Propan-2-ol (500 μl) was added to the supernatant and the tube was inverted and left at room temperature (20 °C) for 10 min. Tubes were centrifuged (21 000 ***g***, 10 min, 4 °C), the supernatant removed, the pellet was washed twice in 80 % ethanol and left to air-dry before being dissolved in diethylpyrocarbonate-treated water. RNA was then purified using the DNA-free kit (Ambion) and RT–PCR carried out using the Promega Access Quick RT–PCR system.

Expression of LKB1 complexes and activation of AMPK-related kinases in HeLa cells

HeLa human cervical carcinoma cells were cultured in DMEM (Dulbecco's modified Eagle's medium) containing 10 % FBS and 1 × penicillin/streptomycin solution (Invitrogen). Cells cultured on 10 cm dishes were transfected with 3 μg of $LKB1_L$ or $LKB1_S$ plasmid and 3 μg of each of FLAG-STRADα and Myc-MO25α plasmids using the polyethylenimine method [35]. The cells were cultured for a further 36 h and lysed in 0.5 ml of ice-cold lysis buffer (50 mM Tris/HCl, pH 7.2, 1 mM EGTA, 1 mM EDTA, 50 mM NaF, 1 mM sodium pyrophosphate, 1 % (w/v) Triton X-100, 0.1 mM PMSF, 1 mM DTT, 0.1 mM benzamidine and 5 μg/ml soybean trypsin inhibitor) after quick rinsing in PBS. The lysates were centrifuged at 4 °C for 10 min at 21 000 ***g***.

For immunoprecipitate kinase assays, 0.1–1 mg of protein was incubated at 4 °C for 2 h on a shaker with 5 μg of the appropriate antibody previously conjugated to 5 μl of Protein G–Sepharose. Kinase activity was then determined as described previously [36] using the AMARA peptide [37] as substrate.

Bacterial expression of the kinase domains of AMPK-α1, BRSK1 and BRSK2

Plasmids encoding GST fusions of the kinase domains of rat AMPK-α1 (residues 1–312), BRSK1 (residues 1–400) and BRSK2 (residues 1–400) were expressed in bacteria from pGEX vectors and purified as described previously [10,38].

Expression of LKB1 in HEK (human embryonic kidney)-293 cells and activation of AMPK-related kinases in cell-free assays

GST–$LKB1_L$ or GST–$LKB1_S$ with FLAG–STRADα and Myc–MO25α were expressed in HEK-293 cells and the complexes purified on glutathione–Sepharose as described previously [39]. GST–AMPKα1, GST–BRSK1 or GST–BRSK2 (1.5 μg in a final volume of 20 μl) were incubated with or without the indicated LKB1 complexes in Buffer A (50 mM Na/Hepes, pH 7.4, 1 mM

DTT and 0.02 % Brij-35) plus 5 mM $MgCl_2$ and 0.2 mM ATP for 15 min at 30 °C. For Western blotting analysis, the reaction was terminated by the addition of LDS sample buffer (Invitrogen). To determine kinase activities, 10 μl was added to 15 μl of mix to give final concentrations of 5 mM $MgCl_2$, 200 μM [γ-^{32}P]ATP (300 c.p.m./pmol) and 200 μM *AMARA* peptide [37] as substrate. After incubation for 15 min at 30 °C, incorporation of ^{32}P-phosphate into the peptide substrate was determined as described previously [40].

Preparation of germ cells from rat testis

Germ cell suspensions were prepared from testes of 26- and 31-day-old Sprague-Dawley rats by collagenase digestion and Percoll purification by a modification of a previous method [41]. In 26-day-old rats, spermatocytes at all phases of the long meiotic prophase are present, and only rare tubules containing young spermatids are seen. In 31-day-old-rats, spermatids are the most prominent germ cell population present. Testes were decapsulated and digested with 0.1 % collagenase (C0130; Sigma-Aldrich) and 0.006 % soybean trypsin inhibitor (T9003; Sigma-Aldrich) in HBSS (Hanks balanced salt solution) for 5 min at room temperature. The collagenase solution was diluted 4-fold with HBSS and seminiferous tubules allowed to sediment for 2 min. The supernatant was discarded and the tubular pellet was washed twice with gentle shaking. Seminiferous tubules were cut into 2 mm segments and then digested with 0.05 % collagenase, 0.003 % soybean trypsin inhibitor and 0.003 % deoxyribonuclease (DN25, Sigma-Aldrich) for 15 min at room temperature, while carefully transferring the suspension from one tube to another with a pipette. The suspension was diluted with one vol. HBSS and material allowed to sediment for 5 min. The supernatant was transferred to a tube containing sufficient 2 % BSA to make the final concentration of 0.2 % BSA. The suspension was allowed to settle for 10 min. Germ cells remaining in suspension were collected by centrifugation at 400 *g* for 3 min at 4 °C. The resulting pellet was washed twice with HBSS containing 0.2 % BSA and 0.003 % deoxyribonuclease. The final cell pellet was resuspended in a 1:1 mixture of DMEM/Ham's F-12 Medium with the addition of 15 mM $NaHCO_3$, 100 IU/ml penicillin, 2.5 mg/ml amphotericin B, 20 mM Na/Hepes, pH 7.4 (DMEM-F12) and seeded on a discontinuous four-layer (20 %, 25 %, 32 %, 37 %) Percoll density gradient. The gradient was centrifuged at 800 ***g*** for 30 min at 4 °C. Two fractions at the 32%–37 % interface and the 25%–32 % interface were collected. To remove Percoll, 4 vol. of DMEM-F12 were added and centrifugation at 400 ***g*** for 5 min at 4 °C performed. Germ cells were resuspended in DMEM-F12 supplemented with 10 mg/ml transferrin, 5 mg/ml insulin, 5 mg/ml vitamin E and 4 ng/ml hydrocortisone. Germ cell preparations were seeded at a density of 2×10^6 cell/ml in tissue culture flasks and cultured at 34 °C in a mixture of 5 % CO_2/95 % air for 18 h. During this initial period, the few Sertoli cells contaminating the germ cell preparation attached to the plastic surface. Purified germ cells were obtained by carefully removing the medium and centrifuging at 400 ***g*** for 5 min at 4 °C. For Western blot analysis, cells were resuspended on ice with 70 ml PBS containing 0.7 ml (per 1×10^6 cells) protease inhibitor cocktail (P8340; Sigma-Aldrich), 2 mM PMSF, 1 mM EGTA, 1 mM EDTA and 1 mM NaF, and disrupted by ultrasonic irradiation. To measure the DNA content, cells were resuspended in DMEM-F12 supplemented with 50 % fetal bovine serum and fixed in ice-cold 70 % ethanol. Propidium iodide was added to fixed cells to a final concentration of 50 mg/ml. Flow cytometry was performed using a FACS Caliber (Becton Dickinson).

Isolation of Leydig cells

Testes from adult Sprague-Dawley rats were removed and placed in ice-cold PBS, pH 7.4, containing 0.1 % BSA. Leydig cells were isolated by a modification of a previous method [42]. Testes were decapsulated and digested with a solution of 0.025 % collagenase (C0130, Sigma–Aldrich) and 0.001 % soybean trypsin inhibitor in M199-BSA (Medium 199 containing 0.1 % BSA) under constant agitation at 34 °C for 15 min. The suspension was diluted 4 times with cold M199-BSA. Seminiferous tubules were allowed to sediment and the supernatant recovered. Seminiferous tubules were washed twice with M199-BSA and supernatants obtained after sedimentation combined with the first supernatant. Interstitial cells were collected by centrifugation at 100 ***g*** for 15 min at 4 °C. Cells were resuspended in DMEM-F12. Leydig cells were purified using a discontinuous four-layer (21 %, 26 %, 40 %, 60 %) Percoll gradient. The gradient was centrifuged at 800 ***g*** for 30 min at 4 °C. The interface between 40 and 60 % Percoll was collected, 4 vol. of DMEM-F12 added, and centrifugation at 400 ***g*** for 5 min at 4 °C was performed. The cell pellets were resuspended on ice with 70 ml PBS containing 0.7 ml (per 1×10^6 cells) protease inhibitor cocktail, 2 mM PMSF, 1 mM EGTA, 1 mM EDTA and 1 mM NaF and disrupted by ultrasonic irradiation.

Isolation of Sertoli cells

Sertoli cells were isolated from 20-day-old Sprague-Dawley rats essentially as previously described [43]. Testes were decapsulated and digested with 0.1 % collagenase (C0130, Sigma-Aldrich) and 0.006 % soybean trypsin inhibitor in HBSS for 5 min at room temperature. Seminiferous tubules were allowed to sediment, washed twice with HBSS, cut into 2mm segments and submitted to treatment with 1 M glycine/2 mM EDTA, 0.003 % deoxyribonuclease, pH 7.4, for 10 min at room temperature to remove peritubular cells. Next, 9 vol. of HBSS were added, and seminiferous tubules were allowed to sediment for 30 min at room temperature. The pellet was recovered and digested again with collagenase under similar conditions for 10 min while carefully transferring the suspension from one tube to another with a pipette. After this, 2 vol. of HBSS were added and Sertoli cell aggregates were collected by centrifugation at 400 ***g*** at 4 °C for 3 min. The pellet obtained was resuspended in HBSS and allowed to settle for 10 min (contaminating germ cells remain in suspension, while Sertoli cell aggregates are recovered in the sediment). The supernatant was discarded and the sediment was washed once with DMEM-F12, collected by centrifugation at 400 ***g*** at 4 °C for 3 min, and finally resuspended in DMEM-F12 supplemented with 10 mg/ml transferrin, 5 mg/ml insulin, 5 mg/ml vitamin E and 4 ng/ml hydrocortisone. Sertoli cells were seeded in a culture dish (60 mg DNA/10 cm^2) and cultured at 34 °C in a mixture of 5 % CO_2/95 % air. The medium was changed after 48 h and cells were collected on day 4, when the purity of Sertoli cells reached 90 % as judged by phase contrast microscopy. Remaining cell contaminants were of germ cell origin. The Sertoli cells were washed once with PBS, collected on ice with 100 ml PBS containing 1 ml protease inhibitor cocktail, 2 mM PMSF, 1 mM EGTA, 1 mM EDTA and 1 mM NaF, and disrupted by ultrasonic irradiation.

Histology of testis and epididymis from LKB1$^{+/+}$ and LKB1$^{fl/fl}$ mice

LKB1$^{+/+}$ and LKB1$^{fl/fl}$ mice were obtained by breeding and genotyping as described previously [44]. Testes and epididymal tissue were dissected and fixed in 10 % neutral buffered formalin overnight. Tissues were embedded in paraffin and sectioned for

standard haematoxylin and eosin staining. Slides were viewed on a Zeiss light microscope, and images taken using a Zeiss Axiocam and processed with AxioVision software.

Sperm counts and assays of sperm motility

Spermatozoa were prepared for counting and motility analysis by macerating the epididymis from $LKB1^{+/+}$ and $LKB1^{fl/fl}$ mice in 200 μl of G-IVF™ PLUS buffer (Vitrolife, Sweden). Tissue was pipetted up and down once or twice, the large tissue fragments allowed to settle and samples of the upper suspension transferred into a clean Eppendorf tube and maintained at 37 °C prior to counting and motility assays. For sperm counts, the sample was diluted 1:5 in water, aliquots (10 μl) pipetted on to an improved Neubauer haemocytometer, and the number of sperm counted using an Olympus IX17 microscope. For motility measurements, 4 μl of the undiluted sample was placed on a glass slide and motility assessed using a computer-aided semen analyser (Hamilton Thorne CEROS) according to manufacturer's instructions.

Microscopic analysis of spermatozoa from $LKB1^{+/+}$ and $LKB1^{fl/fl}$ mice

Spermatozoa were prepared for imaging by finely chopping the epididymis in 4 % paraformaldehyde, which was transferred into a microcentrifuge tube and centrifuged (10000 ***g***, 2 min, 4 °C). The supernatant containing spermatozoa was spotted on to a slide with a drop of Vectashield mounting medium containing DAPI (4′,6-diamidino-2-phenylindole; Vector Labs) and sealed with a coverslip. Images were taken using the bright field and DAPI filter of a Deltavision microscope. Images were also taken using a Nikon Coolpix 4500 digital camera attached to a Zeiss light microscope; sperm counts were taken from these images.

For scanning EM (electron microscopy), the epididymis was finely chopped in Peters fixative (1.25 % glutaraldehyde, 1 % paraformaldehyde, 80 mM Na cacodylate, pH 7.2, 0.02 % $CaCl_2$) and left in fixative overnight. Spermatozoa were collected on 1 μm Shandon Nucleopore membrane filters. After rinsing the membranes twice for 15 min with 80 mM Na cacodylate (pH 7.2), samples were post-fixed with 0.2 % OsO_4 in water overnight. Membranes were washed twice for 15 min in water and then dehydrated through a graded ethanol series. Samples were critically point dried using a BAL-Tec CPD D30, mounted on aluminium stubs using adhesive tabs, and coated with 20 nm Au/Pd using a Cressington 208HR sputter coater. Specimens were examined in a Philips XL30 ESEM operating at an accelerating voltage of 15 Kv, and images recorded using SIS XL DOCU imaging software.

Western blotting and other analytical procedures

SDS/PAGE was performed using precast Bis-Tris 4–12 % gradient polyacrylamide gels in the Mops buffer system (Invitrogen). Proteins were transferred to nitrocellulose membranes (BioRad) using the Xcell II Blot Module (Invitrogen). Membranes were blocked for 1 h in TBS (Tris-buffered saline) containing 5 % (w/v) non-fat dried skimmed milk. The membranes were probed with appropriate antibody (0.1–1 μg/ml) in TBS-Tween and 2 % (w/v) non-fat dried skimmed milk. Detection was performed using secondary antibody (1 μg/ml) coupled to IR 680 or IR 800 dye, and the membranes were scanned using the Li-Cor Odyssey IR imager. Protein concentrations were determined by Coomassie Blue binding [45] with BSA as standard.

RESULTS

Analysis of mRNAs encoding LKB1 by database searching

We previously reported that, during purification from rat liver, two forms of the LKB1–STRAD–MO25 complex could be resolved by anion exchange chromatography, which contained forms of the LKB1 polypeptide with differing mobilities on SDS/PAGE [7]. Since there is a single gene encoding LKB1, we suspected that the two forms might arise by alternative splicing of the mRNA. Using the amino acid sequences for human (Q15831), mouse (Q9WTK7) and rat (XP_234900) LKB1, we searched the respective genome databases and located the sequences on chromosomes 19, 10 and 7 respectively. Each amino acid sequence was aligned against the genomic sequence and intron/exon boundaries identified. We then searched for and aligned ESTs with the genomic sequences. A summary of the alignment is shown in Figure 1(A); the full alignment is available from the authors on request. Interestingly, in all three species, a non-canonical splice site is used for exon 2. A canonical site does exist, and was used in one incorrect prediction for the amino acid sequence of rat LKB1 (XP_234900.1), but every EST found utilizes the non-canonical splice site in all three species.

Our analysis suggested that there are two forms of *LKB1* mRNA caused by alternative splicing after exon 8. These would give rise to two versions of the protein, designated $LKB1_S$ and $LKB1_L$ for the short and long forms respectively, which have different C-terminal sequences encoded by exons 9A and 9B. The $LKB1_L$ mRNA also has an additional exon (exon 10) that encodes a 3′-untranslated sequence only. We also noted the use of alternate polyadenylation sites in exon 10 in both human and mouse. ESTs corresponding to $LKB1_S$ were particularly common in libraries derived from rat testis. In the rat, $LKB1_S$ is predicted to be a protein of 412 amino acid residues with a mass of 46.5 kDa, while $LKB1_L$ is predicted to be a protein of 436 amino acid residues with a mass of 49.2 kDa. The first 373 amino acid residues encoded by exons 1 to 8 (MDVA . . . TVPG), including the kinase domain (44–309), would be identical in both forms. $LKB1_S$ would then have a unique, 39 residue sequence (VEET . . . GAVV) at the C-terminus encoded by exon 9A, whereas $LKB1_L$ would have a unique 63 residue sequence (QVLE . . . CKQQ, including the Ser^{431} phosphorylation site and the cysteine residue in the C-terminal-CAAX sequence that forms the farnesylation site) encoded by exon 9B.

Alignments of the predicted amino acid sequences of the unique C-terminal regions of $LKB1_S$ and $LKB1_L$, encoded by exons 9A and 9B respectively, are shown in Figure 1(B). The unique region of the long form is more highly conserved, being 70 % identical between mouse and human, as opposed to only 36 % identity for the unique region of the short form.

Analysis of LKB1 mRNAs by 3′-RACE

To confirm the existence of two forms of *LKB1* mRNA, we carried out 3′-RACE using cDNA from rat testis as the template, and a forward primer (encoding residues 161–168) derived from the common region. This generated a major product of about 830 bp and a minor product of about 560 bp (results not shown). Sequencing of the 830 bp product yielded a sequence encoding residues 330–412 of $LKB1_S$, covering exons 8 and 9A and extending to the C-terminus of the protein, followed by a TAG stop codon. Sequencing of the 560 bp product yielded a sequence encoding residues 291–406 of $LKB1_L$, including approximately half of the unique C-terminal region. Thus we could distinguish two distinct mRNAs in rat testis mRNA corresponding to $LKB1_S$ and $LKB1_L$.

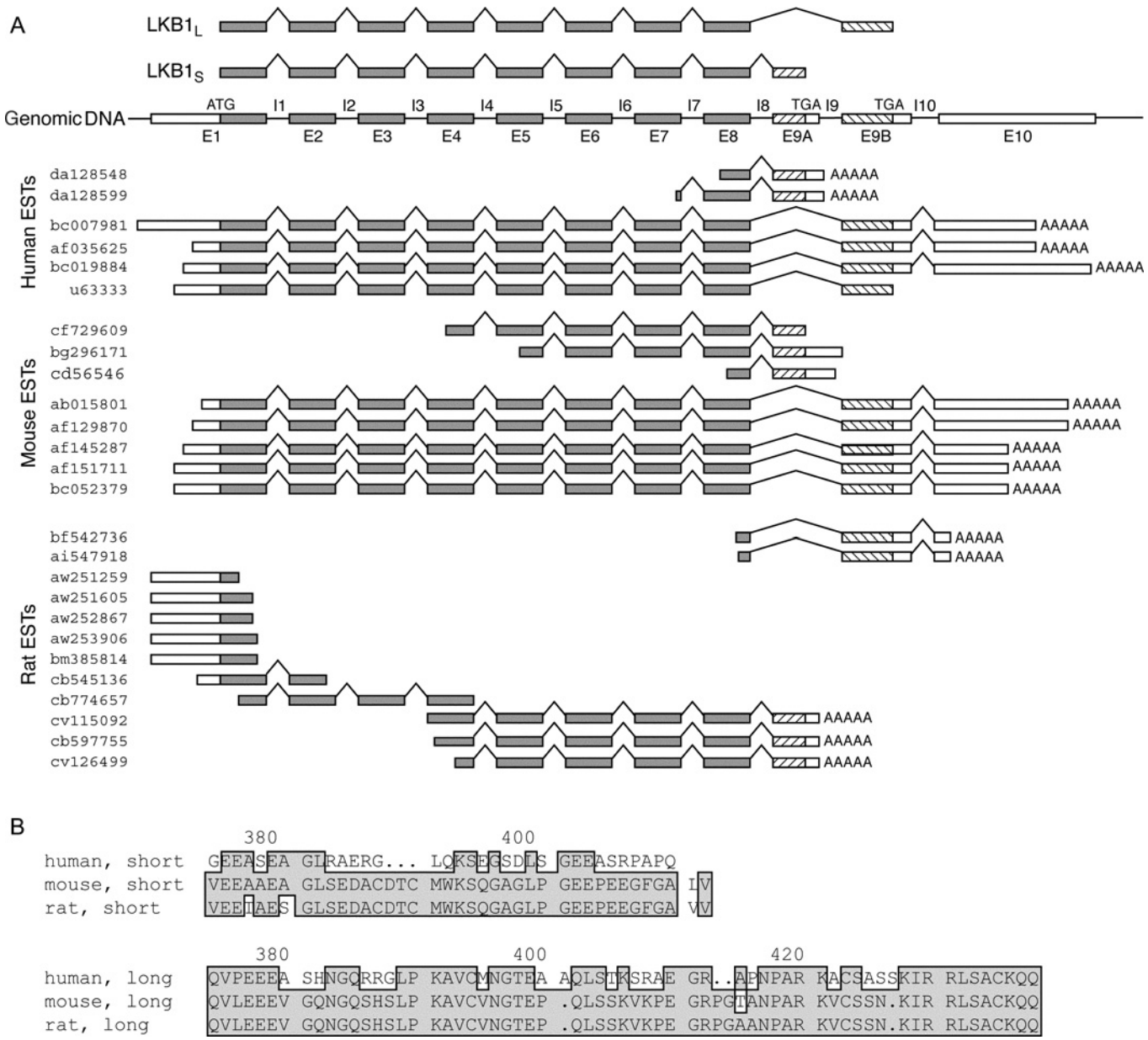

Figure 1 (A) Exon/intron structure of the LKB1 gene and alignment of human, mouse and rat cDNA and EST sequences; (B) alignment of amino acid sequences of the unique C-terminal regions of the short and long forms of LKB1 from human, mouse and rat

(**A**) the arrangement of exons (E1 through E10) and introns (I1 through I10) of the LKB1 gene are shown at the top, and an alignment of cDNA/EST sequences from human, mouse and rat are shown at the bottom. The diagram is not drawn to scale. Protein coding regions common to both isoforms are shown in grey, while the regions in exons 9A and 9B encoding the unique C-terminal regions of $LKB1_S$ and $LKB1_L$ are shown with forward or backward cross-hatching respectively. Database accession numbers are shown at the left. (**B**) Alignment of the unique amino acid sequences of the C-terminal regions of $LKB1_S$ and $LKB1_L$, encoded by exons 9A and 9B, from the human, mouse and rat. Identical residues are marked with grey boxes.

Analysis of $LKB1_S$ and $LKB1_L$ by tryptic peptide mass fingerprinting

To confirm the structural differences between the $LKB1_L$ and $LKB1_S$ at the protein level, we partially purified LKB1 complexes from rat testis and immunoprecipitated them using an antibody, anti-LKB1(N), raised against an epitope (residues 25–36) from the common N-terminal region. SDS/PAGE analysis of the immunoprecipitate revealed five major polypeptides (labelled P1 to P5 in order of increasing mobility, Figure 2A), which had estimated masses by comparison with marker proteins of 50, 46, 43, 40 and 36 kDa. All five were analysed by MALDI–TOF (matrix-assisted laser-desorption ionization–time-of-flight) MS of tryptic peptides. Using this method, P5 was identified as MO25α, and P3 and P4 as STRADα, which has previously been observed to migrate as two or three distinct polypeptides when purified from rat liver [7]. There are two versions of rat STRADα in the NCBI database, i.e. AH81911.1 (GI:51858665), which is predicted to have 373 residues and a mass of 41.4 kDa, and NP_877972.1 (GI:33414519), which is predicted to have 393 residues (including an N-terminal extension not present in

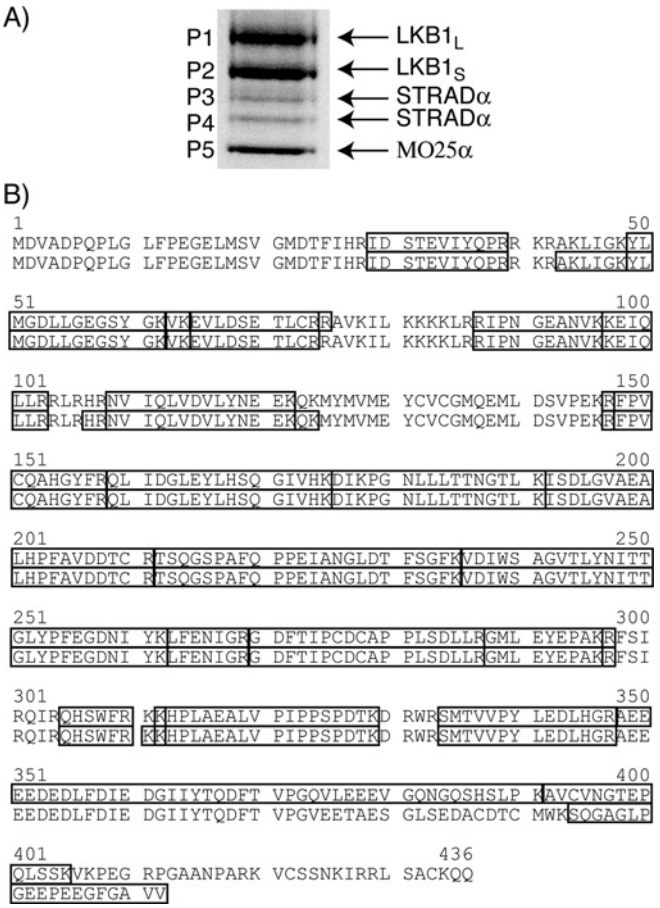

Figure 2 (A) SDS/PAGE analysis of LKB1 purified from rat testis by immunoprecipitation; (B) alignment of predicted amino acid sequences of $LKB1_S$ and $LKB1_L$ with sequence coverage obtained by mass spectrometry

In (**A**), the five major polypeptides detectable by Coomassie Blue staining were identified by MALDI–TOF MS of tryptic peptides. In (**B**), the predicted amino acid sequences of $LKB1_S$ and $LKB1_L$, derived from the analysis shown in Figure 1, were aligned. Boxes indicate tryptic peptides whose masses were identified by MALDI–TOF MS.

AH81911.1) and a mass of 43.5 kDa. P3 and P4 may correspond to these, although we were unable to identify any peptides from the unique N-terminal region of NP_877972.1 in P3.

P1 and P2 were both identified as LKB1. Figure 2(B) shows the complete amino acid sequences of rat $LKB1_S$ and $LKB1_L$ derived from our analysis of DNA sequences in the databases. Tryptic peptides for which we obtained a matching mass in P1 and P2 are indicated by boxes. We identified 17 peptides of the same mass in P1 and P2, accounting for 246 out of 373 residues (64 %) in the N-terminal region common to both variants. In P1 we also identified a peptide of 4949.3 Da, corresponding to residues 348–391 that straddle the junction between exons 8 and 9B, and one of 1504.7 Da, corresponding to residues 392–405 immediately C-terminal to that. Both of these peptides were absent from the digest of P2. Conversely, in P2 we identified a peptide of 1829.9 Da, corresponding to residues 394–412 of the XP_234900.2 sequence, which is the C-terminal peptide of the protein; this peptide was not detected in the digest of P1.

Analysis of $LKB1_S$ and $LKB1_L$ by Western blotting

To study the tissue distribution of LKB1 isoforms at the protein level, we analysed the expression of $LKB1_S$ and $LKB1_L$ in extracts of rat, mouse and human tissues by Western blotting

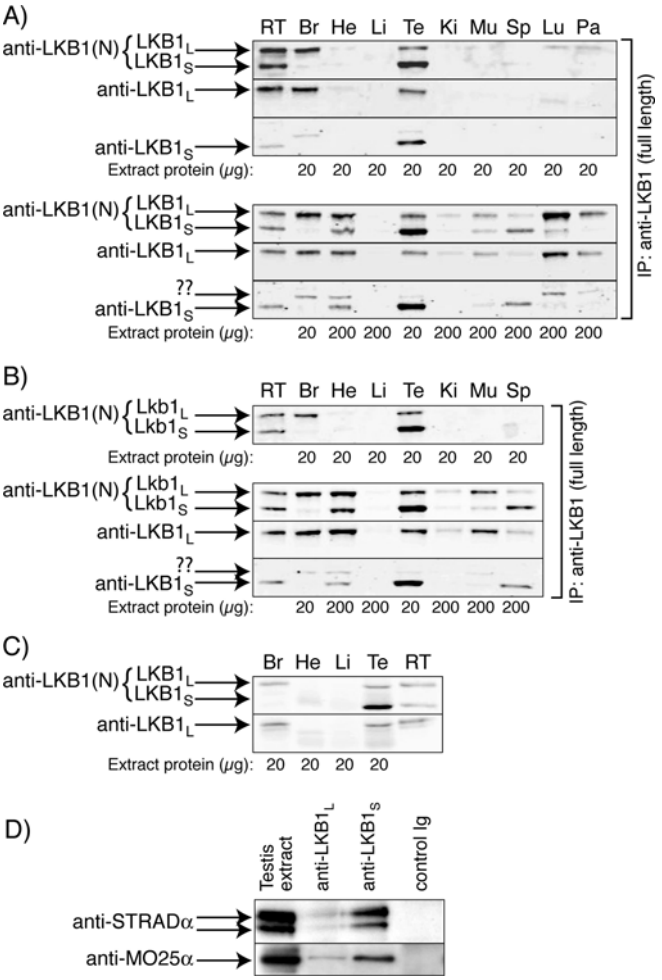

Figure 3 Western blotting of LKB1 polypeptides from extracts of (A) rat, (B) mouse and (C) human, and (D) co-precipitation of STRADα and MO25α with $LKB1_L$ and $LKB1_S$ from rat testis

Key to tissues: RT, purified rat testis enzyme run in each gel as a marker; Br, brain; He, heart; Li, liver; Te, testis; Ki, kidney; Mu, skeletal muscle; Sp, spleen; Lu, lung; Pa, pancreas. For rat and mouse samples, the amount of extract protein shown beneath each lane was immunoprecipitated using an antibody raised against full-length recombinant $LKB1_L$ prior to Western blotting, whereas for human samples, the amount of extract shown was analysed without prior immunoprecipitation. Blots were probed using an antibody against an N-terminal epitope common to both forms [anti-LKB1(N)], or using antibodies against epitopes in the unique C-terminal regions (anti-$LKB1_S$ and anti-$LKB1_L$). The polypeptide labelled '??' is the intermediate band mentioned in the text. For (**D**), immunoprecipitates were made from rat testis extracts using anti-$LKB1_L$, anti-$LKB1_S$ and a control non-immune sheep serum, and analysed by Western blotting using anti-STRADα and anti-MO25α antibodies.

using three different anti-peptide antibodies, i.e. anti-LKB1(N), which recognizes a common N-terminal epitope, and anti-$LKB1_S$ and anti-$LKB1_L$, the latter two raised against C-terminal epitopes that were unique to each variant. To enhance the signals obtained, for rat and mouse extracts we first immunoprecipitated with a fourth antibody made against full-length recombinant $LKB1_L$. Figure 3(A) shows results obtained using rat tissues. If we loaded samples derived from immunoprecipitation of 20 μg of extract protein into each lane, LKB1 polypeptides were only clearly visible in extracts of brain (Br) and testis (Te). The brain sample exhibited only the upper band of 50 kDa recognized by the anti-LKB1(N) and anti-$LKB1_L$ antibodies, while in the testis polypeptides of 50 kDa (recognized by the anti-LKB1(N) and anti-$LKB1_L$ antibodies) and 46 kDa (recognized by the

anti-LKB1(N) and anti-$LKB1_S$ antibodies) were evident. As assessed by the signal obtained using anti-LKB1(N), $LKB1_S$ is more abundant than $LKB1_L$ in testis, although in a sample of partially purified rat testis LKB1 run as a marker (RT), the $LKB1_L$ and $LKB1_S$ polypeptides were of equal intensity.

To examine the expression of the isoforms in other tissues, we ran the Western blots again with the amount of protein increased 10-fold for all tissues except brain and testis. This revealed that both forms were detectable in all tissues examined. Although the signals were very faint for liver (Li) and kidney (Ki), both forms are present in the former because we previously purified them from rat liver [7]. As assessed by the signal obtained using anti-LKB1(N), $LKB1_L$ is more abundant than $LKB1_S$ in brain (Br), heart (He), skeletal muscle (Mu), liver (Li), kidney (Ki), lung (Lu) and pancreas (Pa), whereas the opposite is true in testis (Te) and spleen (Sp). Using the anti-$LKB1_S$ antibody, we also detected an additional polypeptide of intermediate size (labelled "??" in Figure 3A), especially in brain and heart. On close inspection, this could also be seen in the anti-LKB1(N) blots migrating just ahead of $LKB1_L$, but not in the anti-$LKB1_L$ blots. Since this polypeptide was immunoprecipitated using the antibody against full-length LKB1 and is recognized by both anti-LKB1(N) and anti-$LKB1_S$ on Western blots, we suspect that it may represent yet another variant containing the exon 9A sequence. However, we were unable to obtain enough material to confirm this by MS.

Figure 3(B) shows Western blotting of immunoprecipitates of mouse tissue extracts analysed in the same way. Although we did not analyse lung and pancreas, the results were very similar to those obtained with rat extracts, including the putative third variant running between $LKB1_L$ and $LKB1_S$ in brain and heart. Figure 3(C) shows Western blots of extracts of human brain, heart, liver and testis probed with anti-LKB1(N) and anti-LKB_L, with purified rat testis enzyme (RT) run as a positive control. Because the human extracts obtained were already dissolved in SDS, we could not perform prior immunoprecipitation. However, the $LKB1_L$ polypeptide was clearly visible in the brain extract, whereas both $LKB1_L$ and $LKB1_S$ were visible in testis, with $LKB1_S$ being more abundant, as in rodents. Probably because the peptide epitope against which the $LKB1_S$ antibody was made is poorly conserved in humans (Figure 1B), our anti-$LKB1_S$ antibody did not recognize human $LKB1_S$ (results not shown).

To confirm that $LKB1_S$, similarly to $LKB1_L$, formed a complex with STRAD and MO25 in testis, we made rat testis extracts and immunoprecipitated with anti-$LKB1_L$, anti-$LKB1_S$ or with a control sheep immunoglobulin. The extract and each immunoprecipitate was then analysed by Western blotting using antibodies against STRADα and MO25α. The results (Figure 3D) confirmed that both $LKB1_L$ and $LKB1_S$ formed complexes with STRADα and MO25α in testis. Two polypeptides of 43 and 40 kDa were observed for STRADα as in Figure 2. Although the STRAD and MO25 polypeptides were only faintly detected in the anti-$LKB1_L$ blots due to the low expression of this variant in testis, we have previously shown that $LKB1_L$ associates with STRADα and MO25α in rat liver [7].

Subcellular localization of $LKB1_S$ and $LKB1_L$

Since $LKB1_S$ lacks the C-terminal -CKQQ sequence providing the cysteine that is farnesylated on $LKB1_L$ [31], we wondered whether the two isoforms might have different subcellular localizations. However, after expression of $LKB1_L$ or $LKB1_S$ in HeLa cells with or without STRADα and MO25α, with detection by indirect immunofluorescence using isoform-specific antibodies, or by Western blotting after separation of extracts into soluble and membrane fractions, we could obtain no evidence that this was the case. These results are presented in the Supplementary Data section (http://www.BiochemJ.org/bj/416/bj4160001add.htm, Figure S1).

$LKB1_S$ and $LKB1_L$ activate AMPK and AMPK-related kinases

To determine whether both variants of LKB1 are capable of activating AMPK and the AMPK-related kinases in intact cells, we co-expressed $LKB1_L$ or $LKB1_S$ with FLAG–STRADα and Myc–MO25α in HeLa cells and measured the phosphorylation and activity of endogenous kinases compared with untransfected controls. By probing blots with the anti-LKB1(N) antibody, the expression of $LKB1_L$ was higher than that of $LKB1_S$ in these cells (Figure 4A). Despite this, endogenous AMPK was activated and phosphorylated to approximately equal extents compared with control cells treated with empty vector (Figure 4B). Similar results were obtained with SIK1 (SIK), SIK2 (QIK), SIK3 (QSK) and NUAK2 [SNARK (SNF1/AMP-activated related protein kinase)]: in these cases the basal activity in control cells was very low and there was a large increase in activity upon expression of either splice variant (Figures 4C–4F).

As the brain-specific kinases BRSK1 and BRSK2 (also known as SAD-B and SAD-A) are not expressed in HeLa cells, we used a different approach to assess their phosphorylation and activation by $LKB1_L$ and $LKB1_S$ complexes. We co-expressed GST-tagged $LKB1_L$ or $LKB1_S$ in HEK-293 cells with FLAG–STRAD-α and Myc–MO25α and purified the recombinant complexes using glutathione–Sepharose chromatography. Figure 5(A) shows analysis of the purified complexes by blotting with anti-GST, -FLAG and -Myc antibodies. This shows that the LKB1–STRADα–MO25α complex was highly enriched in the glutathione–Sepharose eluate. The bottom panel of Figure 5(A) shows a Western blot probed with anti-GST using a lighter loading of the purified complex, revealing that the content of $LKB1_L$ and $LKB1_S$ in the two preparations was equivalent.

As an initial test of this method, we examined the ability of the purified $LKB1_L$ and $LKB1_S$ complexes to phosphorylate and activate a GST fusion of the kinase domain from rat AMPK-α1. Both complexes were active, but the $LKB1_S$ complex appeared to activate the α1 kinase domain, and phosphorylate Thr^{172}, more effectively than the $LKB1_L$ complex (Figures 5B and 5C). Similar results were obtained with GST–BRSK1 and GST–BRSK2, although there were quantitative differences, with the $LKB1_S$ complex appearing to phosphorylate and activate BRSK2 much more efficiently than the $LKB1_L$ complex (Figures 5E and 5G), whereas this difference was less marked with BRSK1 (Figures 5D and 5F).

A role for $LKB1_S$ in spermiogenesis

We used a mouse with a 'floxed' *Lkb1* gene to investigate the function of $LKB1_S$. This mouse carries an allele of *Lkb1* in which exons 4 to 8 have been replaced by a cDNA-IRES NEO-loxP(3′) cassette; the cDNA encodes exons 5, 6, 7, 8 and 9b of $Lkb1_l$ [44]. Although the genome of these mice still contains the exon 9a sequence, this was not likely to be transcribed as part of the *Lkb1* transcript because the cDNA cassette is already spliced and carries polyadenylation sequences. Therefore these homozygous floxed mice ($Lkb1^{fl/fl}$) should represent a *de facto* knockout of $Lkb1_S$. To confirm this at the mRNA level, we extracted RNA from rat testis and used it as a template for RT–PCR using forward primers from the region common to $Lkb1_L$ and $Lkb1_S$ and reverse primers from their unique 3′ regions (expected size of products 592 and 609 bp respectively). We also used primers to amplify 18S rRNA as a positive control. The results (Figure 6A) showed that mRNA encoding $Lkb1_S$ was completely absent in the

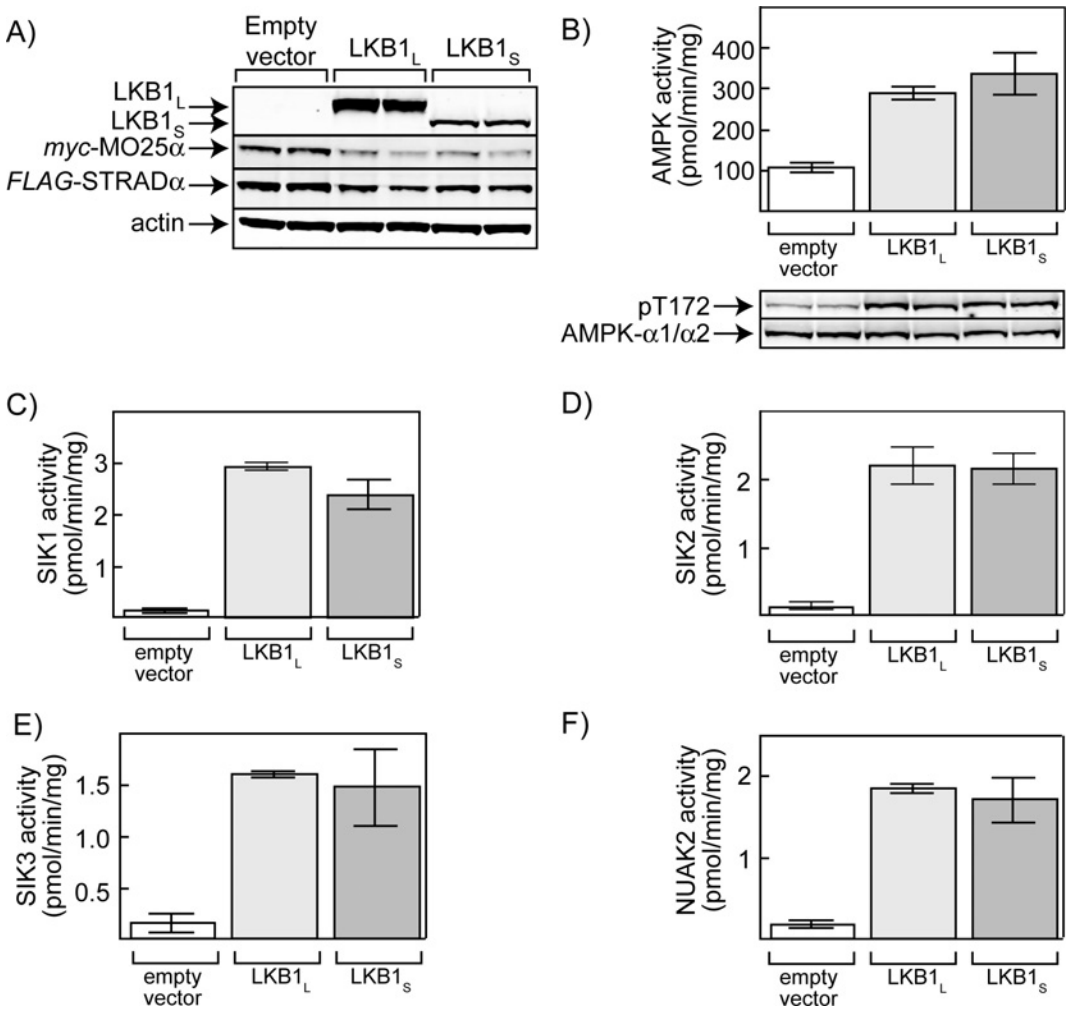

Figure 4 Activation of endogenous AMPK and AMPK-related kinases in HeLa cells transfected with or without $LKB1_L$ or $LKB1_S$ plus myc-MO25α and FLAG-STRADα

(**A**) Cell lysates were blotted with anti-$LKB1_L$, anti-$LKB1_S$, anti-Myc or anti-FLAG antibodies. (**B**) The activity of endogenous AMPK was assayed after immunoprecipitation with a mixture of anti-AMPK-α1 and-α2 antibodies, and the phosphorylation and expression of AMPK determined by Western blotting with anti-pT172 (anti-phosphoTyr^{172}) and a mixture of anti-AMPK-α1 and -α2 antibodies. (**C**–**F**) The activities of endogenous SIK1, SIK2, SIK3 and NUAK2 were assayed after immunoprecipitation with anti-SIK1, -SIK2, -SIK3 and -NUAK2 antibodies.

RNA from the homozygous floxed mice, which still contained both $Lkb1_L$ mRNA and 18S rRNA. To confirm the absence of $Lkb1_S$ in the homozygous floxed mice at the protein level, we also carried out Western blotting with increasing amounts of testis protein (Figure 6B).

The *Lkb1*$^{fl/fl}$ mice have no overt phenotype, other than that the male mice are sterile [44]. Our current findings, that $Lkb1_S$ is expressed at highest levels in the testis and is absent in the testis of the *Lkb1*$^{fl/fl}$ males, suggests that this variant might play a crucial role in spermatogenesis. We first looked at the expression of $Lkb1_S$ and $Lkb1_L$ in different regions of the male reproductive system in wild-type mice. Expression of $Lkb1_S$, measured either using the antibody specific for that variant (anti-$LKB1_S$) or the antibody that recognizes both variants [anti-LKB1(N)] was very high in the testis but much lower in the epididymis and in spermatozoa derived from epididymis (Figure 6C). By contrast, $Lkb1_L$ appeared to be expressed at low levels in all three preparations. This suggested that $Lkb1_S$ might have a function in developing, rather than in mature, spermatozoa.

We next examined the expression of $LKB1_S$ in testis from rats of different ages (Figure 6D). $LKB1_S$ expression was absent in testis from rats that were 20, 23 and 27 days old, but was evident in 30-day-old rats and much stronger in 60-day-old rats. The expression of LKB1 therefore corresponds to the time (day 27) when haploid spermatids begin to appear. We also examined expression in Leydig cells (LC), Sertoli cells (SC) and three different preparations of germ cells (G1, G2, G3) made by collagenase digestion and Percoll gradient centrifugation of rat testis (Figure 6E). $LKB1_S$ was clearly expressed in whole testis, with the expression being greater in 60-day-old rather than 30-day-old rats as before. It was expressed in germ cells but not in Leydig or Sertoli cells. However, expression varied markedly in the three different preparations of germ cells. Preparation G1 was from 26-day-old rats (32–37 % Percoll interface), contained 75 % tetraploid cells and 6 % haploid cells and expressed no detectable $LKB1_S$. Preparation G2 was from 26-day-old rats (25–32 % Percoll interface), contained 73 % tetraploid cells and 16 % haploid cells and expressed low levels of $LKB1_S$. Preparation G3 was from 31-day-old rats, contained 27 % tetraploid cells and 63 % haploid cells and expressed high levels of $LKB1_S$. Thus the highest expression of $LKB1_S$ appears to be in developing germ cells after meiosis. All three germ cell preparations contained

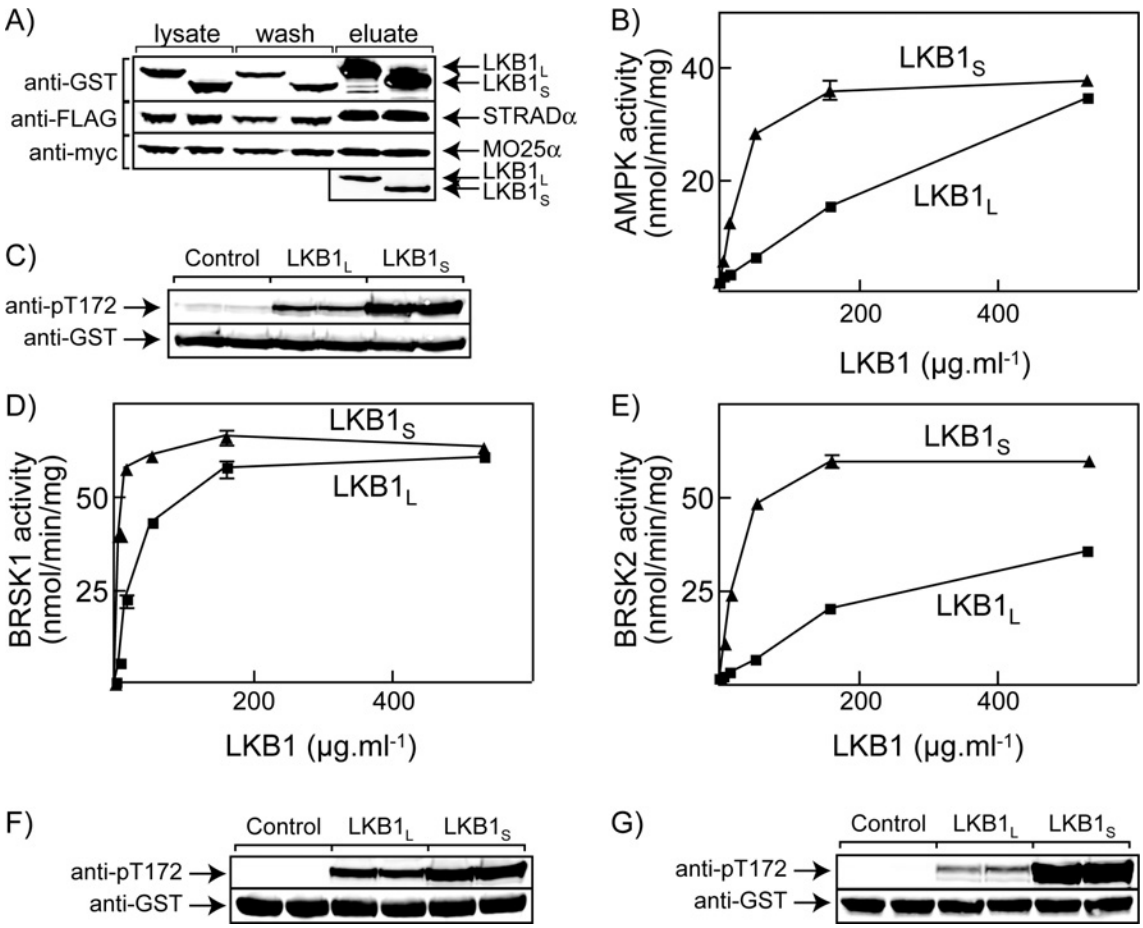

Figure 5 Activation of purified GST fusions of AMPK (α1 kinase domain, residues 1–312), BRSK1 and BRSK2 by recombinant GST–LKB1:FLAG–STRADα:Myc–MO25α complexes expressed in HEK-293 cells

(**A**) Western blotting using the indicated antibodies on HEK-293 cell lysates, the initial wash of the glutathione–Sepharose column, and the glutathione eluate; the bottom panel shows a lower loading of the glutathione eluate probed with anti-GST to show equal recovery of $LKB1_L$ and $LKB1_S$. (**B**) Activation of bacterially-expressed GST–AMPK-α1 kinase domain using various concentrations of the recombinant LKB1 complexes shown in (**A**). (**C**) Phosphorylation of GST–AMPK-α1 kinase domain using 1 in 5 dilutions of the recombinant LKB1 complexes, assessed using anti-pT172 antibody, with anti-GST antibody used for loading controls. (**D**) and (**F**), as (**B**) and (**C**), but using GST–BRSK1 in place of GST–AMPK-α1 kinase domain. (**E**) and (**G**), as (**B**) and (**C**), but using GST–BRSK2 in place of GST–AMPK-α1 kinase domain. The results for (**B**), (**D**) and (**E**) show mean $\pm$ range of duplicate observations. Where error bars are not visible they lie within the symbol. These experiments were performed twice with very similar results.

small proportions of diploid cells (10–20 %) that may represent contamination with somatic cells.

We also analysed the testis and epididymis, and the spermatozoa stored in the latter, from the mice that lacked $Lkb1_S$ and their wild-type littermates. Histological analyses using haematoxylin and eosin staining of testis sections did not reveal any marked differences (results not shown), but there were obvious differences in the epididymis. Whereas the caudal region (where mature spermatozoa are stored) was distended and packed with spermatozoa in the wild type, it appeared to be shrunken and almost empty in the *Lkb1*$^{fl/fl}$ mice (Figure 7). To recover the spermatozoa we finely chopped the whole epididymis, resuspended in buffer used for motility analysis of human spermatozoa, allowed the large tissue fragments to settle, and counted spermatozoa. This revealed that the number of mature spermatozoa was drastically reduced in the *Lkb1*$^{fl/fl}$ mice. In six *Lkb1*$^{fl/fl}$ mice of ages ranging from 2 to 12 months, the sperm count was reduced by 98.6 $\pm$ 1.0 % compared with their wild-type littermates. Analysis of motility revealed that the spermatozoa from the wild-type littermates had normal motility ($\approx$ 67 % motile with 28 % progressive), but that the few spermatozoa from the *Lkb1*$^{fl/fl}$ mice were completely non-motile. In addition, the few spermatozoa that were recovered from the knockout mice had an abnormal morphology. Viewed by differential bright field microscopy or by scanning EM, the sperm heads from the wild type littermates had the characteristic hooked shape caused by the prominent acrosome in mouse spermatozoa. However, the sperm heads from the *Lkb1*$^{fl/fl}$ mice were invariably rounded and showed no evidence of the hooked acrosome. In addition, the chromatin appeared to be less highly condensed than in wild-type sperm heads as judged by staining of DNA in fluorescence microscopy (Figure 7).

DISCUSSION

The first indication that LKB1 might exist as two protein variants came from studies showing that the LKB1 complex could be separated into two fractions during purification from rat liver [7]. When we searched cDNA databases from rat, mouse and human, we found sequences corresponding to two distinct forms of LKB1 mRNA (Figure 1A), with many of the cDNAs corresponding

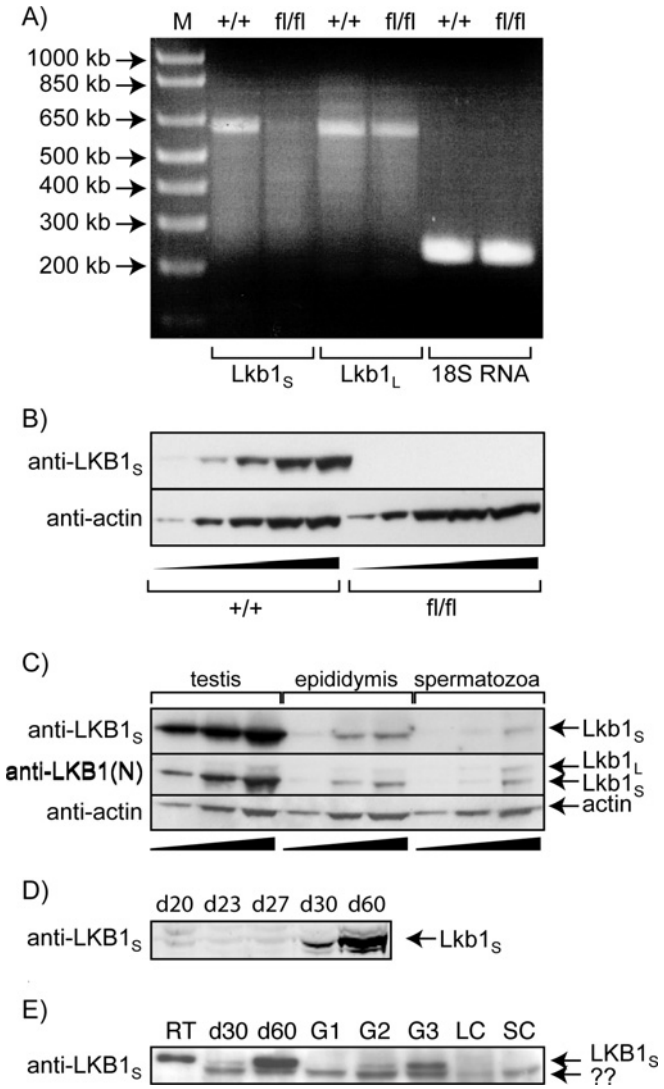

Figure 6 Lack of expression of $LKB1_S$ in $LKB1^{fl/fl}$ mice at the (A) RNA and (B) protein level; (C) expression of $LKB1_L$ and $LKB1_S$ in testis, epididymis and in mature spermatozoa from wild-type mice; and expression of $LKB1_S$ in whole testis (D) and different testis cell types (E) from rats of different ages

(**A**) mRNAs encoding $LKB1_L$ and $LKB1_S$, and 18S rRNA, were amplified by RT–PCR using appropriate primers from testis of wild-type (+/+) and floxed (fl/fl) mice; the left-hand lane contains molecular mass markers (M) of the indicated size. (**B**) Western blots with increasing amounts of total testis protein from wild-type (+/+) and floxed (fl/fl) mice; blots were also probed with anti-actin antibodies as a loading control. (**C**) Increasing loadings of extract protein from testis, epididymis and spermatozoa from wild-type mice were analysed by Western blotting using anti-$LKB1_S$, anti-LKB1(N) and anti-actin antibodies. (**D**) Western blots of testis extracts (30 μg protein) from rats of different ages (d20–d60: 20-, 23-, 27-, 30- and 60-day-old). (**E**) Analysis of purified rat testis LKB1, whole testis from 30-day-old (d30) and 60-day-old (d60) rats, three different preparations of testis germ cells (G1, G2, G3), Leydig cells (LC) and Sertoli cells (SC). Samples contained 60 μg of total protein, except for the purified rat testis LKB1, which was 20 μg. Germ cell fractions G1 and G2 were from 26-day-old rats and were recovered at the 32–37% and the 25–32% Percoll interfaces respectively. Fraction G3 was from 31-day-old rats and was recovered at the 25–32% Percoll interface. By flow cytometry, the proportions of cells with 4n, 2n and 1n DNA content were G1: 75%, 19%, 6%; G2: 73%, 11%, 16% and G3: 27%, 10%, 63%. The expression of $LKB1_S$ therefore correlates with the proportion of haploid cells.

to the short form (particularly in the case of the rat) being derived from the testis. This is consistent with our findings that mRNAs encoding two distinct forms of LKB1 could be cloned by a 3′-RACE procedure from rat testis cDNA and could also be detected by RT–PCR (Figure 6A). To confirm expression of both variants at the protein level, we partially purified LKB1 from rat testis extracts and immunoprecipitated using an antibody that recognizes both forms. This resulted in the identification by peptide mass fingerprinting of $LKB1_L$, $LKB1_S$, MO25α and two forms of STRADα. Thus, the existence of the two splice variants of LKB1 was demonstrated unequivocally at the protein level in rat testis.

We next examined the tissue distribution of the two splice variants in rat, mouse and human extracts using an antibody raised against an N-terminal epitope expected to recognize both forms [anti-LKB1(N)] and two antibodies raised against unique sequences encoded by exons 9B (anti-$LKB1_L$) and 9A (anti-$LKB1_S$). In most tissue extracts, $LKB1_L$ was the predominant form, although $LKB1_S$ was always detectable if sufficient protein was loaded onto the gel. The exceptions to this were spleen extracts from rats and mice (a human spleen sample was not available) and testis extracts from all three species, where $LKB1_S$ was the predominant form. $LKB1_S$ was much more abundant in testis than any other tissue extract, whereas $LKB1_L$ was most abundant in brain extracts.

We next considered the possibility that the unique C-terminal regions of $LKB1_L$ and $LKB1_S$ might provide docking sites such that they would differ in their specificity for the downstream protein kinases. To test this, we co-expressed $LKB1_L$ and $LKB1_S$ in HeLa cells, which do not express endogenous LKB1, with FLAG–STRADα and Myc–MO25α and assessed the activation state of AMPK and AMPK-related kinases (SIK1, SIK2, SIK3 and NUAK2/SNARK). We also studied the activation of AMPK, BRSK1/SAD-B and BRSK2/SAD-A by recombinant $LKB1_L$ and $LKB1_S$ complexes in cell-free assays. Our results did not support the idea that the two splice variants have intrinsic specificity for any of the downstream targets.

Recently, a conditional mouse model of the *Lkb1* gene has been generated [44,46]. Although exon 9A is still present in the genome of $Lkb1^{fl/fl}$ mice, it can no longer be transcribed as part of the *Lkb1* mRNA, abrogating production of the $LKB1_S$ variant. This was confirmed in the present study both by RT–PCR and by Western blotting (Figure 6). These mice do not have an obvious developmental phenotype, other than the sterility of the $Lkb1^{fl/fl}$ male mice. In wild-type mice, we found that expression of $Lkb1_S$ was particularly high in the testis where spermatozoa are developing, and then dropped markedly in the epididymis (where mature spermatozoa are stored) as well as in the mature spermatozoa themselves. In contrast, the expression of $Lkb1_L$ was low and uniform in all stages (Figure 6C). Analysis by Western blotting of different cell types prepared from rat testis showed that $LKB1_S$ was expressed at high levels in germ cells but not in Leydig or Sertoli cells. Moreover, in different preparations of germ cells, $LKB1_S$ expression was much higher in those that had a high proportion of cells with haploid (1n) DNA content and a low proportion of tetraploid (4n) DNA content. These haploid cells represent early, round spermatids and have not yet undergone the dramatic changes in cell polarity that occur during spermiogenesis, including the formation of the acrosome body at the sperm head, growth of the sperm tail, the formation of the mid-piece containing mitochondria, and the compaction of chromatin.

The most striking differences between the $Lkb1^{fl/fl}$ mice (which are $Lkb1_S$ knockouts) and their wild-type littermates were in the epididymis, and particularly in the caudal (tail) region where mature spermatozoa are stored. While the tubule in the caudal region of the wild-type was distended and packed with spermatozoa, in the knockouts the tubule was shrunken and appeared to be almost empty. Consistent with this, the numbers

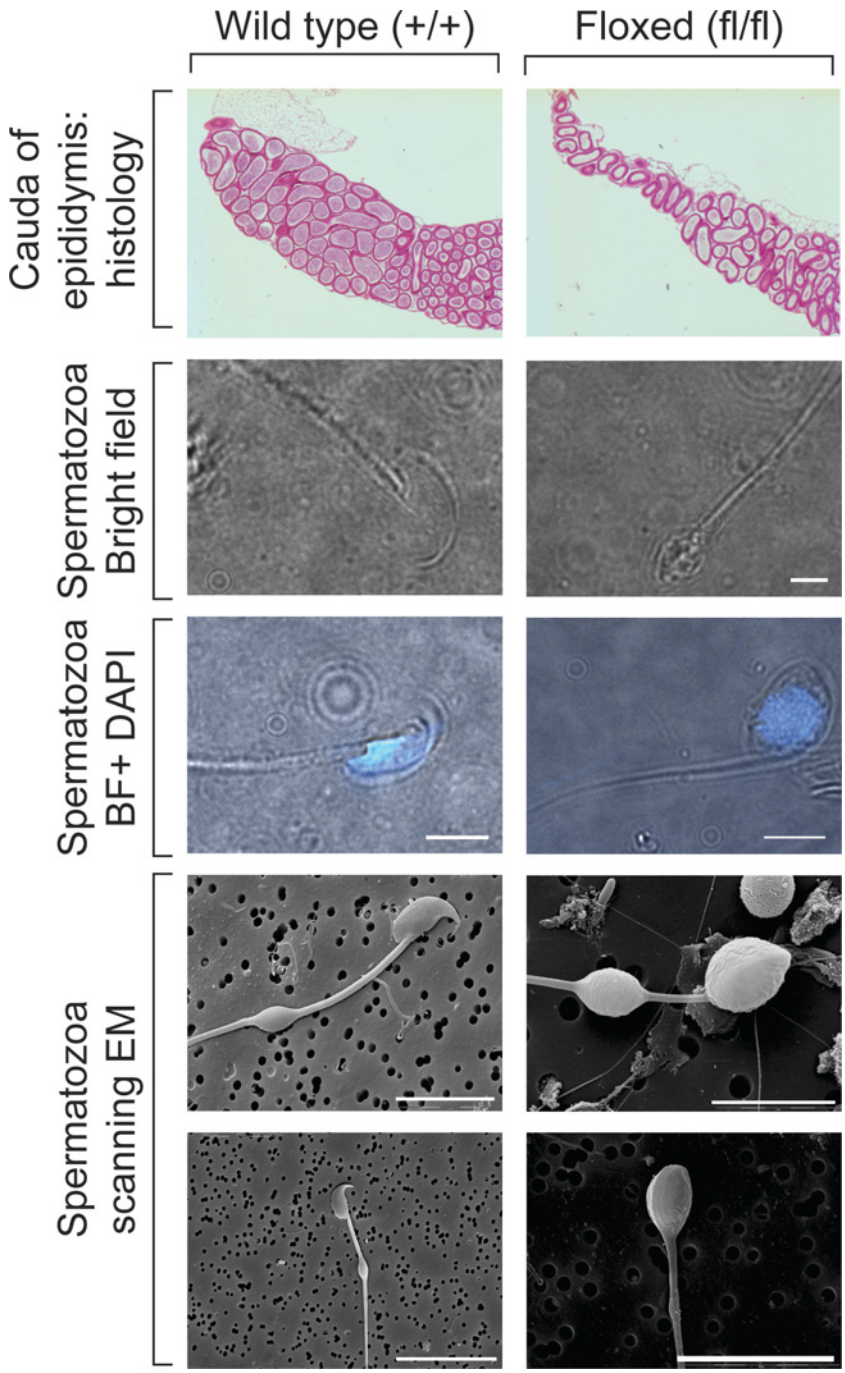

Figure 7 Histology of the cauda of the epididymis, and bright field (BF) microscopy and scanning EM of spermatozoa from wild-type (+/+) and LKB1 floxed (fl/fl) mice

In the panels third from top, the cells were stained with DAPI to reveal DNA and the pictures represent merged bright field and fluorescence images. The epididymis contains spermatozoa at different stages of maturation, and in some (see upper scanning EM images) the cytoplasmic droplet has not been completely absorbed. Both the histology and the scanning EM were performed with wild-type and LKB1 floxed mice of various ages (2 months, $n=2$; 5 months, $n=3$; 12 months, $n=1$). The results were very similar in every case. The scanning EM pictures are representative of several spermatozoa examined from each epididymis, although the number recovered from the the LKB1 floxed animals was very small.

of spermatozoa that we could recover from the epididymis, in mice ranging from 2 to 12 months, were reduced by >98 %. In addition, those few spermatozoa that were recovered were non-motile and had grossly abnormal morphology. Although they still had tails, the sperm heads were rounded and lacked the characteristic hooked shape provided by the acrosome of mouse spermatozoa. The heads were also larger and it appeared that the chromatin was less highly condensed (Figure 7). Although we have not established the molecular basis for these defects, our results suggest that $Lkb1_S$ is required for the process of spermiogenesis. This may reflect a specialized example of the role of LKB1 and AMPK in establishment of cell polarity, since spermiogenesis is one of the most dramatic examples of cell polarization. However, the possibility that abnormal regulation

of one of the other AMPK-related kinases may play a role in this phenotype should also be considered.

We also addressed the question of whether our discovery of the novel splice variant had implications for PJS. Almost all of the reported PJS mutations distal to the kinase domain (none of which appear to prevent association with STRAD or MO25 or abolish kinase activity [47]) occur in exon 8, so would affect both $LKB1_L$ and $LKB1_S$. This includes the P324L, F354L and T367M mutations that have recently been reported to retain the ability to cause growth arrest in G361 cells, while being impaired in activation of AMPK and inhibition of the TOR pathway, and in the induction of polarity in intestinal cells and astrocytes [48]. One possible exception is a mutation that converts codon 416 in exon 9B (AAG, encoding Lys^{416}) to a TAG stop codon [49], which would remove the last 18 residues of $LKB1_L$, including the Ser^{431} phosphorylation site and the farnesylated cysteine. This appeared to cause classical, familial PJS where the patient had multiple intestinal polyps, suggesting that PJS can occur with a mutation that would not affect $LKB1_S$. However, it has not been ruled out whether there might have been additional mutations in exon 9A in this case. A related question is whether any PJS mutations might occur in exon 9A. Up to 20 % of subjects with PJS have no known mutation in the *LKB1* gene but, prior to this study, exon 9A had not been recognized as an important part of the gene and may not have been sequenced in DNA from PJS subjects. However, sequencing of exon 9A in DNA from 13 individuals where no other mutations have been found did not reveal any new mutations (V. Launonen and L. Aaltonen, personal communication).

In conclusion, we have discovered a novel splice variant of LKB1, termed $LKB1_S$, that is particularly expressed in early spermatids prior to spermiogenesis, the process in which the highly polarized structures of spermatozoa are formed. Male mice that represent a *de facto* knockout of $Lkb1_S$ form very small numbers of polarized spermatozoa that have abnormal heads. Our results suggest that $LKB1_S$ has an essential role in spermiogenesis and male fertility.

ACKNOWLEDGEMENTS

We thank Professor Dario Alessi (MRC Protein Phosphorylation Unit, University of Dundee, Dundee, U.K.) for antibodies and helpful discussions, Dr Keith Baar (Division of Molecular Physiology, University of Dundee) for primers against 18S RNA, Martin Kierans, John James and Calum Thomson at the Centre for High Resolution Imaging and Processing at the University of Dundee for help with scanning EM and histology, and Chris Barratt and Lindsay Tulloch for help with the sperm counts and assays of motility. We are very grateful to Virpi Launonen and Lauri Aaltonen for sequencing exon 9A DNA from PJS subjects.

FUNDING

This study was supported by a Programme Grant from the Wellcome Trust [grant number 80982], by Cancer Research U.K. [grant number C347/A8363] and Breakthrough Breast Cancer, by the EXGENESIS Integrated Project [grant number LSHM-CT-2004-005272] from the European Commission and by the pharmaceutical companies that support the Division of Signal Transduction Therapy (AstraZeneca, Boehringer-Ingelheim, GlaxoSmithKline, Merck & Co., Merck KGaA and Pfizer).

REFERENCES

1 Hemminki, A., Markie, D., Tomlinson, I., Avizienyte, E., Roth, S., Loukola, A., Bignell, G., Warren, W., Aminoff, M., Hoglund, P. et al. (1998) A serine/threonine kinase gene defective in Peutz-Jeghers syndrome. Nature **391**, 184–187

2 Jenne, D. E., Reimann, H., Nezu, J., Friedel, W., Loff, S., Jeschke, R., Muller, O., Back, W. and Zimmer, M. (1998) Peutz-Jeghers syndrome is caused by mutations in a novel serine threonine kinase. Nat. Genet. **18**, 38–43

3 Alessi, D. R., Sakamoto, K. and Bayascas, J. R. (2006) Lkb1-dependent signaling pathways. Annu. Rev. Biochem. **75**, 137–163

4 Watts, J. L., Morton, D. G., Bestman, J. and Kemphues, K. J. (2000) The *C. elegans* par-4 gene encodes a putative serine-threonine kinase required for establishing embryonic asymmetry. Development **127**, 1467–1475

5 Martin, S. G. and St Johnston, D. (2003) A role for Drosophila LKB1 in anterior-posterior axis formation and epithelial polarity. Nature **421**, 379–384

6 Lee, J. H., Koh, H., Kim, M., Kim, Y., Lee, S. Y., Karess, R. E., Lee, S. H., Shong, M., Kim, J. M., Kim, J. and Chung, J. (2007) Energy-dependent regulation of cell structure by AMP-activated protein kinase. Nature **447**, 1017–1020

7 Hawley, S. A., Boudeau, J., Reid, J. L., Mustard, K. J., Udd, L., Makela, T. P., Alessi, D. R. and Hardie, D. G. (2003) Complexes between the LKB1 tumor suppressor, STRADα/β and MO25α/β are upstream kinases in the AMP-activated protein kinase cascade. J. Biol. **2**, 28

8 Shaw, R. J., Kosmatka, M., Bardeesy, N., Hurley, R. L., Witters, L. A., DePinho, R. A. and Cantley, L. C. (2004) The tumor suppressor LKB1 kinase directly activates AMP-activated kinase and regulates apoptosis in response to energy stress. Proc. Natl. Acad. Sci. U.S.A. **101**, 3329–3335

9 Woods, A., Johnstone, S. R., Dickerson, K., Leiper, F. C., Fryer, L. G., Neumann, D., Schlattner, U., Wallimann, T., Carlson, M. and Carling, D. (2003) LKB1 is the upstream kinase in the AMP-activated protein kinase cascade. Curr. Biol. **13**, 2004–2008

10 Lizcano, J. M., Göransson, O., Toth, R., Deak, M., Morrice, N. A., Boudeau, J., Hawley, S. A., Udd, L., Mäkelä, T. P., Hardie, D. G. and Alessi, D. R. (2004) LKB1 is a master kinase that activates 13 protein kinases of the AMPK subfamily, including the MARK/PAR-1 kinases. EMBO J. **23**, 833–843

11 Jaleel, M., McBride, A., Lizcano, J. M., Deak, M., Toth, R., Morrice, N. A. and Alessi, D. R. (2005) Identification of the sucrose non-fermenting related kinase SNRK, as a novel LKB1 substrate. FEBS Lett. **579**, 1417–1423

12 Hardie, D. G. (2007) AMP-activated/SNF1 protein kinases: conserved guardians of cellular energy. Nat. Rev. Mol. Cell Biol. **8**, 774–785

13 Inoki, K., Zhu, T. and Guan, K. L. (2003) TSC2 mediates cellular energy response to control cell growth and survival. Cell **115**, 577–590

14 Gwinn, D. M., Shackelford, D. B., Egan, D. F., Mihaylova, M. M., Mery, A., Vasquez, D. S., Turk, B. E. and Shaw, R. J. (2008) AMPK phosphorylation of raptor mediates a metabolic checkpoint. Mol. Cell **30**, 214–226

15 Imamura, K., Ogura, T., Kishimoto, A., Kaminishi, M. and Esumi, H. (2001) Cell cycle regulation via p53 phosphorylation by a 5′-AMP activated protein kinase activator, 5-aminoimidazole- 4-carboxamide-1-beta-d-ribofuranoside, in a human hepatocellular carcinoma cell line. Biochem. Biophys. Res. Commun. **287**, 562–567

16 Jones, R. G., Plas, D. R., Kubek, S., Buzzai, M., Mu, J., Xu, Y., Birnbaum, M. J. and Thompson, C. B. (2005) AMP-activated protein kinase induces a p53-dependent metabolic checkpoint. Mol. Cell **18**, 283–293

17 Shaw, R. J., Bardeesy, N., Manning, B. D., Lopez, L., Kosmatka, M., DePinho, R. A. and Cantley, L. C. (2004) The LKB1 tumor suppressor negatively regulates mTOR signaling. Cancer Cell **6**, 91–99

18 Huang, X., Wullschleger, S., Shpiro, N., McGuire, V. A., Sakamoto, K., Woods, Y. L., McBurnie, W., Fleming, S. and Alessi, D. R. (2008) Important role of the LKB1-AMPK pathway in suppressing tumorigenesis in PTEN-deficient mice. Biochem. J. **412**, 211–221

19 Baas, A. F., Kuipers, J., van der Wel, N. N., Batlle, E., Koerten, H. K., Peters, P. J. and Clevers, H. C. (2004) Complete polarization of single intestinal epithelial cells upon activation of LKB1 by STRAD. Cell **116**, 457–466

20 Zheng, B. and Cantley, L. C. (2007) Regulation of epithelial tight junction assembly and disassembly by AMP-activated protein kinase. Proc. Natl. Acad. Sci. U.S.A. **104**, 819–822

21 Zhang, L., Li, J., Young, L. H. and Caplan, M. J. (2006) AMP-activated protein kinase regulates the assembly of epithelial tight junctions. Proc. Natl. Acad. Sci. U.S.A. **103**, 17272–17277

22 Drewes, G., Ebneth, A., Preuss, U., Mandelkow, E. M. and Mandelkow, E. (1997) MARK, a novel family of protein kinases that phosphorylate microtubule-associated proteins and trigger microtubule disruption. Cell **89**, 297–308

23 Kishi, M., Pan, Y. A., Crump, J. G. and Sanes, J. R. (2005) Mammalian SAD kinases are required for neuronal polarization. Science **307**, 929–932

24 Sapkota, G. P., Deak, M., Kieloch, A., Morrice, N., Goodarzi, A. A., Smythe, C., Shiloh, Y., Lees-Miller, S. P. and Alessi, D. R. (2002) Ionizing radiation induces ataxia telangiectasia mutated kinase (ATM)-mediated phosphorylation of LKB1/STK11 at Thr-366. Biochem. J. **368**, 507–516

25 Sugden, C., Crawford, R. M., Halford, N. G. and Hardie, D. G. (1999) Regulation of spinach SNF1-related (SnRK1) kinases by protein kinases and phosphatases is associated with phosphorylation of the T loop and is regulated by 5′-AMP. Plant J. **19**, 433–439

26 Woods, A., Salt, I., Scott, J., Hardie, D. G. and Carling, D. (1996) The α1 and α2 isoforms of the AMP-activated protein kinase have similar activities in rat liver but exhibit differences in substrate specificity *in vitro*. FEBS Lett. **397**, 347–351

27 Goransson, O., McBride, A., Hawley, S. A., Ross, F. A., Shpiro, N., Foretz, M., Viollet, B., Hardie, D. G. and Sakamoto, K. (2007) Mechanism of action of A-769662, a valuable tool for activation of AMP-activated protein kinase. J. Biol. Chem. **282**, 32549–32560
28 Baas, A. F., Boudeau, J., Sapkota, G. P., Smit, L., Medema, R., Morrice, N. A., Alessi, D. R. and Clevers, H. C. (2003) Activation of the tumour suppressor kinase LKB1 by the STE20-like pseudokinase STRAD. EMBO J. **22**, 3062–3072
29 Altschul, S. F., Madden, T. L., Schaffer, A. A., Zhang, J., Zhang, Z., Miller, W. and Lipman, D. J. (1997) Gapped BLAST and PSI-BLAST: a new generation of protein database search programs. Nucleic Acids Res. **25**, 3389–3402
30 Clamp, M., Cuff, J., Searle, S. M. and Barton, G. J. (2004) The Jalview Java alignment editor. Bioinformatics **20**, 426–427
31 Sapkota, G. P., Kieloch, A., Lizcano, J. M., Lain, S., Arthur, J. S., Williams, M. R., Morrice, N., Deak, M. and Alessi, D. R. (2001) Phosphorylation of the protein kinase mutated in Peutz-Jeghers cancer syndrome, LKB1/STK11, at Ser431 by p90(RSK) and cAMP-dependent protein kinase, but not its farnesylation at Cys(433), is essential for LKB1 to suppress cell growth. J. Biol. Chem. **276**, 19469–19482
32 Boudeau, J., Deak, M., Lawlor, M. A., Morrice, N. A. and Alessi, D. R. (2003) Heat-shock protein 90 and Cdc37 interact with LKB1 and regulate its stability. Biochem. J. **370**, 849–857
33 Pozuelo Rubio, M., Geraghty, K. M., Wong, B. H., Wood, N. T., Campbell, D. G., Morrice, N. and Mackintosh, C. (2004) 14-3-3-affinity purification of over 200 human phosphoproteins reveals new links to regulation of cellular metabolism, proliferation and trafficking. Biochem. J. **379**, 395–408
34 Williamson, B. L., Marchese, J. and Morrice, N. A. (2006) Automated identification and quantification of protein phosphorylation sites by LC/MS on a hybrid triple quadrupole linear ion trap mass spectrometer. Mol. Cell. Proteomics **5**, 337–346
35 Durocher, Y., Perret, S. and Kamen, A. (2002) High-level and high-throughput recombinant protein production by transient transfection of suspension-growing human 293-EBNA1 cells. Nucleic Acids Res. **30**, E9
36 Hardie, D. G., Salt, I. P. and Davies, S. P. (2000) Analysis of the role of the AMP-activated protein kinase in the response to cellular stress. Methods Mol. Biol. **99**, 63–75
37 Dale, S., Wilson, W. A., Edelman, A. M. and Hardie, D. G. (1995) Similar substrate recognition motifs for mammalian AMP-activated protein kinase, higher plant HMG-CoA reductase kinase-A, yeast SNF1, and mammalian calmodulin-dependent protein kinase I. FEBS Lett. **361**, 191–195
38 Scott, J. W., Norman, D. G., Hawley, S. A., Kontogiannis, L. and Hardie, D. G. (2002) Protein kinase substrate recognition studied using the recombinant catalytic domain of AMP-activated protein kinase and a model substrate. J. Mol. Biol. **317**, 309–323
39 Boudeau, J., Baas, A. F., Deak, M., Morrice, N. A., Kieloch, A., Schutkowski, M., Prescott, A. R., Clevers, H. C. and Alessi, D. R. (2003) MO25a/b interact with STRADa/b enhancing their ability to bind, activate and localize LKB1 in the cytoplasm. EMBO J. **22**, 5102–5114
40 Davies, S. P., Carling, D. and Hardie, D. G. (1989) Tissue distribution of the AMP-activated protein kinase, and lack of activation by cyclic AMP-dependent protein kinase, studied using a specific and sensitive peptide assay. Eur. J. Biochem. **186**, 123–128
41 Schteingart, H. F., Rivarola, M. A. and Cigorraga, S. B. (1989) Hormonal and paracrine regulation of gamma-glutamyl transpeptidase in rat Sertoli cells. Mol. Cell. Endocrinol. **67**, 73–80
42 Dufau, M. L., Mendelson, C. R. and Catt, K. J. (1974) A highly sensitive *in vitro* bioassay for luteinizing hormone and chorionic gonadotropin: testosterone production by dispersed Leydig cells. J. Clin. Endocrinol. Metab. **39**, 610–613
43 Meroni, S. B., Riera, M. F., Pellizzari, E. H. and Cigorraga, S. B. (2002) Regulation of rat Sertoli cell function by FSH: possible role of phosphatidylinositol 3-kinase/protein kinase B pathway. J. Endocrinol. **174**, 195–204
44 Sakamoto, K., McCarthy, A., Smith, D., Green, K. A., Hardie, D. G., Ashworth, A. and Alessi, D. R. (2005) Deficiency of LKB1 in skeletal muscle prevents AMPK activation and glucose uptake during contraction. EMBO J. **24**, 1810–1820
45 Bradford, M. M. (1976) A rapid and sensitive method for the quantitation of microgram quantities of protein utilizing the principle of protein-dye binding. Anal. Biochem. **72**, 248–254
46 Sakamoto, K., Zarrinpashneh, E., Budas, G. R., Pouleur, A. C., Dutta, A., Prescott, A. R., Ashworth, A., Jovanovic, A., Alessi, D. R. and Bertrand, L. (2006) Deficiency of LKB1 in heart prevents ischemia-mediated activation of AMPKα2 but not AMPKα1. Am. J. Physiol. Endocrinol. Metab. **290**, E780–E788
47 Boudeau, J., Scott, J. W., Resta, N., Deak, M., Kieloch, A., Komander, D., Hardie, D. G., Prescott, A. R., van Aalten, D. M. and Alessi, D. R. (2004) Analysis of the LKB1-STRAD-MO25 complex. J. Cell Sci. **117**, 6365–6375
48 Forcet, C., Etienne-Manneville, S., Gaude, H., Fournier, L., Debilly, S., Salmi, M., Baas, A., Olschwang, S., Clevers, H. and Billaud, M. (2005) Functional analysis of Peutz-Jeghers mutations reveals that the LKB1 C-terminal region exerts a crucial role in regulating both the AMPK pathway and the cell polarity. Hum. Mol. Genet. **14**, 1283–1292
49 Wang, Z. J., Churchman, M., Avizienyte, E., McKeown, C., Davies, S., Evans, D. G., Ferguson, A., Ellis, I., Xu, W. H., Yan, Z. Y. et al. (1999) Germline mutations of the LKB1 (STK11) gene in Peutz-Jeghers patients. J. Med. Genet. **36**, 365–368

Received 17 July 2008/3 September 2008; accepted 5 September 2008
Published as BJ Immediate Publication 5 September 2008, doi:10.1042/BJ20081447

Biochem. J. (2008) **416**, 1–14 (Printed in Great Britain) doi:10.1042/BJ20081447

SUPPLEMENTARY ONLINE DATA

A novel short splice variant of the tumour suppressor LKB1 is required for spermiogenesis

Mhairi C. TOWLER*, Sarah FOGARTY*, Simon A. HAWLEY*, David A. PAN*[2], David M. A. MARTIN†, Nicolas A. MORRICE‡, Afshan McCARTHY§, María N. GALARDO‖, Silvina B. MERONI‖, Selva B. CIGORRAGA‖, Alan ASHWORTH§, Kei SAKAMOTO‡ and D. Grahame HARDIE*[1]

*Division of Molecular Physiology, School of Life Sciences, University of Dundee, Dow Street, Dundee DD1 5EH, Scotland, U.K., †Post-Genomics and Molecular Interactions Centre, College of Life Sciences, University of Dundee, Dundee DD1 5EH, Scotland, U.K., ‡MRC Protein Phosphorylation Unit, College of Life Sciences, University of Dundee, Dundee DD1 5EH, Scotland, U.K., §The Breakthrough Breast Cancer Research Centre, The Institute of Cancer Research, Fulham Road, London SW3 6JB, U.K., and ‖Centro de Investigaciones Endocrinológicas (CEDIE-CONICET), Hospital de Niños "R. Gutiérrez", Gallo 1330, C1425EFD Buenos Aires, Argentina

MATERIALS AND METHODS

Subcellular localization of LKB1 variants in HeLa and NG108 cells

Easy T HeLa cells and NG108 cells were cultured in DMEM supplemented with 10 % foetal bovine serum. Cells were transfected using Superfect transfection reagent (Qiagen). For immunofluorescence, cells grown on cover slips were transfected and 24 h later were processed as follows. Cells were washed in PBS, fixed in 4 % paraformaldehyde and washed in PBS before being permeabilized in 0.2 % (v/v) Triton X-100 in PBS. Cells were washed in PBS prior to incubation in blocking solution, 0.2 % fish skin gelatin (Sigma) in PBS. Primary and secondary antibodies were diluted in blocking solution and incubated with cells for 20 min each, with washes between incubations. Cover slips were mounted in Vectashield containing DAPI (Vector Laboratories). All steps were performed at room temperature. Images were acquired on a Deltavision restoration microscope (Applied Precision Instruments, Issaquah, WA, U.S.A.) running SoftWoRx (Applied Precision) deconvolution and data analysis software.

Subcellular fractionation of HeLa and NG108 cell lysates

Membrane and cytosol fractions were prepared from HeLa and NG108 neuroblastoma cells that had been transfected using Superfect (Qiagen), with plasmids encoding $LKB1_L$ or $LKB1_S$ plus STRADα and MO25α. Cells were lysed in lysis buffer (50 mM Tris/HCl, pH 7.5, 1 mM EGTA, 1 mM EDTA, 1 mM $NaVO_4$, 50 mM NaF, 0.27 M sucrose, 0.1 % 2-mercaptoethanol plus protease inhibitors) for 30 min on ice, followed by 30 strokes with a Dounce homogenizer, and the homogenates were centrifuged (1500 ***g***; 10 min; 4 °C). The supernatants were transferred into fresh tubes and centrifuged again (10000 ***g***, 10 min, 4 °C). The supernatants were centrifuged again (150000 ***g***, 1.5 h, 4 °C) and the supernatants defined as the cytosol fraction. The membrane pellet was resuspended in lysis buffer containing 1 % Triton X-100 for 20 min at 4 °C and defined as the membrane fraction. Equal amounts of protein were separated by SDS/PAGE, and Western blots probed using anti-LKB1(N).

RESULTS

Subcellular localization of $LKB1_S$ and $LKB1_L$

Since $LKB1_S$ lacks the -CKQQ sequence at the C-terminus that provides the cysteine that is farnesylated on $LKB1_L$ [1], we wondered whether the two isoforms might have different subcellular localizations. To address this, we initially expressed $LKB1_S$ and $LKB1_L$ in HeLa cells (which lack expression of endogenous LKB1) with or without STRADα and MO25α, and the cells were fixed and stained using the antibodies against the unique C-terminal regions of the two isoforms. This revealed that, as reported previously for $LKB1_L$ [2], both isoforms were localized in the nucleus when expressed on their own, but re-localized to the cytoplasm when co-expressed with STRADα and MO25α (Figure S1A). No signal was obtained when mock-transfected cells were probed, or when cells transfected with $LKB1_L$ were probed with the anti-$LKB1_S$ antibody, or vice versa (results not shown), confirming the specificity of the antibodies, at least in these cells. Both $LKB1_S$ and $LKB1_L$ were rather diffusely distributed in the cytoplasm when co-expressed with STRADα and MO25α, although there appeared to be some enrichment in membrane protrusions, particularly for $LKB1_S$ (yellow arrow in the top-right panel of Figure S1A). These protrusions appear to represent lamellipodia involved in cell migration across the culture dish.

We also prepared soluble and membrane fractions from the transfected HeLa cells and probed blots using anti-LKB1(N), which recognizes both forms of LKB1. This revealed that, although only $LKB1_L$ contains the farnesylation sequence at the C-terminus, both forms were predominantly recovered in the cytoplasmic fraction with only a small proportion in the membrane fraction (Figure S1B). Very similar results were obtained in the NG108 neuroblastoma-glioma cell line. However, we were also able to detect endogenous $LKB1_L$ (but not $LKB1_S$) in NG108 cells using this antibody, and the distribution of the endogenous protein between the soluble and membrane fractions was approximately equal. Moreover, the $LKB1_L$ polypeptide migrated with a lower mobility in the membrane fraction. This difference could be due either to differential farnesylation, or to differential phosphorylation of Ser^{431}, because it has previously been shown that only membrane-bound LKB1 is phosphorylated at this site in Rat-2 fibroblast cells [1].

[1] To whom correspondence should be addressed (email d.g.hardie@dundee.ac.uk).
[2] Present address: Prosidion Limited, Windrush Court, Watlington Road, Oxford OX4 6LT, U.K.

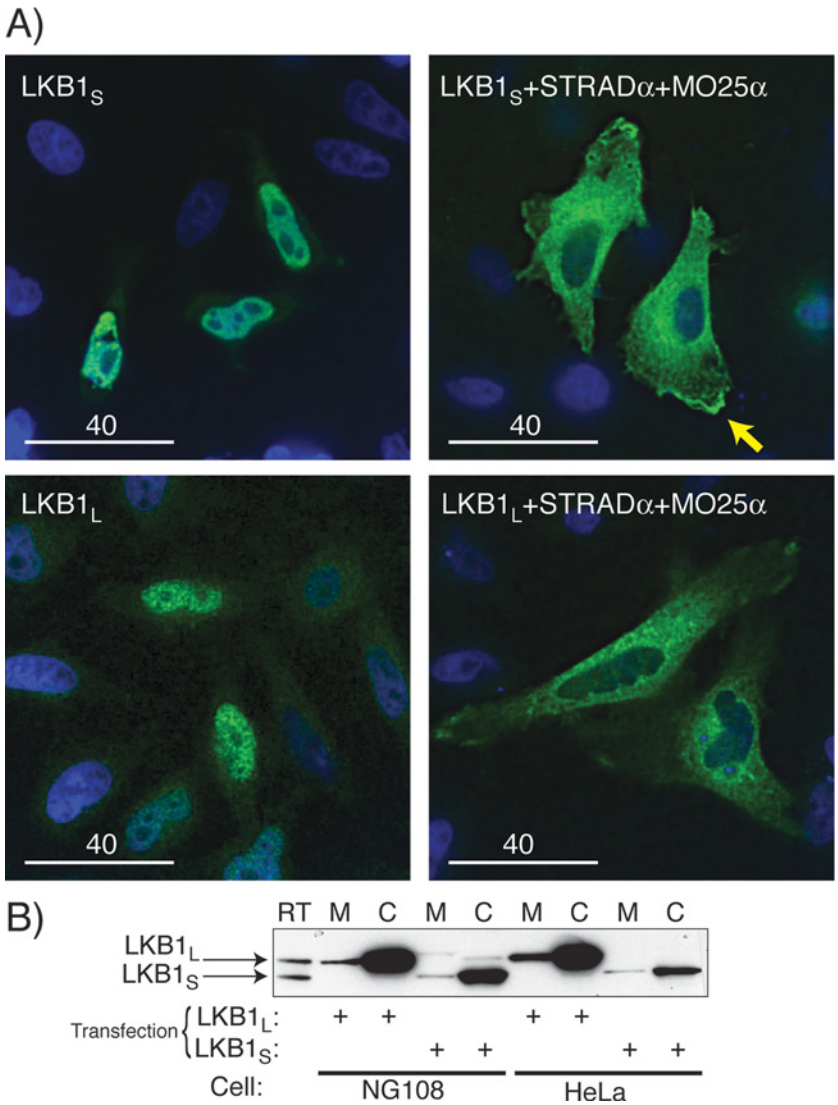

Figure S1 (A) Subcellular localization of expressed $LKB1_L$ and $LKB1_S$ in HeLa cells; and (B) distribution of $LKB1_L$ and $LKB1_S$ between membrane and cytosol fractions in HeLa and NG108 cells

In (**A**), cells were transfected with the plasmids shown, and fixed and permeabilized cells were probed with anti-$LKB1_S$ (upper panels) or anti-$LKB1_L$ (lower panels). Antibody staining is shown in green, and staining with DAPI reveals the nuclei in blue. The yellow arrow in the top-right panel shows the apparent enrichment of $LKB1_S$ in membrane protrusions. Untransfected cells gave no signal with anti-$LKB1_S$ or anti-$LKB1_L$, nor did cells transfected with $LKB1_S$ (with or without STRADα and MO25α) and probed with anti-$LKB1_L$, or cells transfected with $LKB1_L$ (with or without STRADα and MO25α) and probed with anti-$LKB1_S$ (not shown). In (**B**), membrane (M) and cytosol (C) fractions were prepared from NG108 and HeLa cells that had been transfected with plasmids encoding $LKB1_L$ or $LKB1_S$, STRADα and MO25α, and were analysed by Western blotting using anti-LKB1(N) antibody. A sample of purified rat testis LKB1 (RT) was run as a positive control.

REFERENCES

1 Sapkota, G. P., Kieloch, A., Lizcano, J. M., Lain, S., Arthur, J. S., Williams, M. R., Morrice, N., Deak, M. and Alessi, D. R. (2001) Phosphorylation of the protein kinase mutated in Peutz-Jeghers cancer syndrome, LKB1/STK11, at Ser431 by p90(RSK) and cAMP-dependent protein kinase, but not its farnesylation at Cys(433), is essential for LKB1 to suppress cell growth. J. Biol. Chem. **276**, 19469–19482

2 Boudeau, J., Baas, A. F., Deak, M., Morrice, N. A., Kieloch, A., Schutkowski, M., Prescott, A. R., Clevers, H. C. and Alessi, D. R. (2003) MO25a/b interact with STRADa/b enhancing their ability to bind, activate and localize LKB1 in the cytoplasm. EMBO J. **22**, 5102–5114

Received 17 July 2008/3 September 2008; accepted 5 September 2008
Published as BJ Immediate Publication 5 September 2008, doi:10.1042/BJ20081447